

東海大學環境科學與工程學系碩士班

碩士論文

利用可回收之磁性鈀-錳催化劑降解天然有機物及模
式之建立

**Apply and modelling recyclable magnetic
palladium-manganese catalyst with ozonation to
decompose natural organic matters**

指導教授：張鎮南 博士

研究生：曹佳茹 撰

中華民國 104 年 2 月

東海大學碩士班研究生
論文指導教授推薦書

環境科學與工程學系 曹佳茹君所提之論文

題目：利用可回收之磁性鈀-錳催化劑降解天然有機物及模式之建立

Apply and modelling recyclable magnetic palladium-manganese
catalyst with ozonation to decompose natural organic matters

係由本人指導撰述，同意提付審查。

指導教授： 張穎南 (簽章)

104年1月21日

東海大學環境科學系碩士班

論文口試委員審定書

環境科學與工程學系碩士班曹佳茹君所提之論文

題目：利用可回收之磁性鈀-錳催化劑降解天然有機物及模式之建立

Apply and modelling recyclable magnetic palladium-manganese catalyst with ozonation to decompose natural organic matters

經本委員會審議，認為符合碩士資格標準。

論文口試委員召集人 李益浩 (簽章)

委員 張耀南

王學康
陳谷汎

中華民國 104 年 2 月 10 日

致謝

在研究所的生活中，很感謝張鎮南 教授的悉心指導，給予機會進入實驗室裡做研究並提供良好的研究環境，以及不時討論並給予研究方向使我學習到很多知識。同時謝謝宋孟浩 老師、王繁慷 老師和陳谷汎 老師在百忙之中擔任學生的論文口試委員並給予許多指正及教導。

兩年多來的日子，實驗室裡共同的生活點滴，學術上的討論，一起趕報告的革命情感，讓我的碩士生活多采多姿，非常感謝實驗室裡的夥伴們，慧燕學姊的幫助及鼓勵，理維學長、宣根學長、祐祺學長、硯勳學長，在實驗及論文上的指導及幫忙；謝謝志哲的共同砥礪，也謝謝學弟妹：文志、哲豪、及大學部的依庭、欣宜、雅萍、佩萱、苓菱，同時也謝謝其他實驗室的同學們一起加油打氣，使我的碩士生涯不孤單且絢麗。

另外，還要感謝我的男朋友康甫，謝謝你從大學以來的支持與陪伴，陪我度過許多難關，並給我一隻寶貝兔兒子小肥，陪我度過寫論文的孤單夜晚。

最後更要感謝我的家人，感謝在天上的爸爸的保佑，也謝謝我親愛的媽媽以妹妹們，你們的支持、關心及體諒，讓我有堅持到最後的毅力，我畢業了，謝謝大家。

摘要

本研究利用浸漬法合成磁性鈇-錳顆粒($\text{Fe}_3\text{O}_4/\text{SiO}_2/\text{Pd-Mn}$)進行催化臭氣之實驗，並利用 X-射線繞射分析(XRD)、掃描電子顯微鏡(SEM)及能量散佈分析儀(EDS) 觀察其催化劑之表面特徵分析。由 SEM 圖像顯示鈇-錳催化劑為球型顆粒其粒徑約為 50-100 奈米，EDS 的元素分析及 XRD 圖譜證明鈇及錳元素皆有確實塗覆在催化劑上，其鈇和錳的含量分別為 1.66%、2.4%。鈇-錳催化劑進行異相催化臭氣處理台中中部德基水庫原水，並探討水中 A_{254} 和 DOC 之降解變化。催化劑濃度在 1g/L 具有良好的去除效率， A_{254} 降解率及 DOC 的礦化率分別達到 70% 和 60%，而 pH 11 下，其 A_{254} 去除率及 DOC 的礦化率更能達到 80% 及 90% 左右。以一階反應方程式之 k_d (反應衰變速率常數) 值比較，發現使用催化臭氣之 k_d 值($k_d = 6.5 \times 10^{-2}$) 高於其他文獻之 k_d 值。香豆素作為捕捉氫氧自由基的物質，7-香豆素為降解香豆素之中間產物，實驗數據顯示出在 pH 11 時，降解效率高，其 k 值為 $6.0 \times 10^{-2} \text{ min}^{-1}$ ，7-香豆素的濃度也最高間接證明，在此條件下產生較多氫氧自由基。而以最佳條件下降解三鹵甲烷生成之前驅物，結果顯示催化臭氣後其去除率(74%)高於單獨臭氣(38%)，在回收實驗中，其降解率能保持在 80% 左右。實驗數據(A_{254} and THMFP) 可使用發展修改的 Nernst 方程式。結果顯示鈇-錳催化劑能有效降解天然有機物。

關鍵字:催化臭氣、天然有機物、Nernst 程式、鈀-錳、回收



Abstract

This study synthesized magnetic $\text{Fe}_3\text{O}_4/\text{SiO}_2/\text{Pd-Mn}$ catalysts in an ozonation system by the impregnation method. Catalysts were characterized using X-ray diffraction (XRD), scanning electron microscope (SEM) and Energy Dispersive Spectrometer (EDS). From the electron microscope image of the appearance of spherical catalyst particles was with diameter around 50-100 nm. The output of XRD and EDS showed that palladium and manganese were coated on the particle properly and the weight percent of palladium and manganese in the catalyst were 1.66% and 2.4%, respectively. It was used to decompose natural organic matters (NOMs) which were the water resource from central Taiwan, the Te-Chi reservoir. Heterogeneous catalytic ozonation in this study was investigated the degradation efficiency of DOC and A_{254} . With the dose of 1 g/L of catalyst, the system can reach the decomposition of A_{254} and DOC to 70% and 60% respectively. While with the same dose under pH 11 case, the decay rate of A_{254} and DOC upgrade to 80% and 90% simultaneously. The first order reaction kinetic rates ($k_d = 6.5 \times 10^{-2}$) indicated the catalyst can provide strong removal capability of NOMs compared to that reported in the literature.

Coumarin is a scavenger in catalytic ozonation to capture free radical in solution. At pH 11, it has more efficient to decompose coumarin in the reactor, and k value obtained $6.0 \times 10^{-2} \text{ min}^{-1}$. The generation of by-product: 7-hydroxycoumarin had been indicated the effect of hydroxyl radical. At pH 11, the amount of 7-hydroxycoumarin had been generated mostly compared with other conditions of pH. The ratio of decomposition of THMFPS in catalytic ozonation had 74% more than 38% by sole ozonation. The recycle catalysts conduct the similar ozone test and can remain 80% removal efficiency. The experimental data (A_{254} and THMFP) are used to develop a modified Nernst type model for heterogeneous catalytic ozonation. The results indicated $\text{Fe}_3\text{O}_4/\text{SiO}_2/\text{Pd-Mn}$ catalyst can effectively degrade natural organic matter.

Keywords

Catalytic ozonation, Natural organic matters, Nernst equation, Pd-Mn, recycle.

CONTENTS

CONTENTS	VI
Table List	IX
Figure List.....	IX
Chapter 1 Introduction.....	1
1.1 Research Background.....	1
1.2 Objectives.....	4
Chapter 2 Literature Review.....	5
2.1 Natural Organic Matters (NOMs) in water	5
2.2 Disinfection by-products (DBPs).....	9
2.3 Advanced Oxidation Processes (AOPs).....	10
2.3.1 Ozone reaction.....	12
2.3.2 Catalytic ozonation.....	14
2.3.2.1 Homogeneous catalytic ozonation.....	15
2.3.2.2 Heterogeneous catalytic ozonation.....	17
2.4 Catalyst.....	20
2.4.1 Metal oxide and metal oxide on support.....	20
2.4.2 Nanoparticles and nanocatalysts.....	21
2.4.3 Pd-Mn catalysts.....	22
2.5 Hydroxyl radical scavengers.....	23
Chapter 3 Material and Methods.....	25
3.1 Experiment Frameworks.....	25
3.2 Sample Preparation and Fractionation Procedures.....	27
3.2.1 Sampling Site and Preservation.....	27
3.2.2 Extraction procedure.....	28
3.3 Preparation of catalyst.....	34
3.3.1 Synthesis of Fe ₃ O ₄	34
3.3.2 Synthesis of Fe ₃ O ₄ /SiO ₂	34

3.3.3	Synthesis of Fe ₃ O ₄ /SiO ₂ /Pd-Mn.....	35
3.4	Ozonation and Catalytic Ozonation System.....	37
3.5	Analysis Methods.....	40
3.5.1	Basic water quality analysis.....	40
3.5.2	Disinfection By-Product Formation Potential (DBPFP) Study.....	41
3.5.3	Trihalomethanes (THMs).....	41
3.5.4	The Characteristics of Fe ₃ O ₄ /SiO ₂ /Pd-Mn.....	43
3.5.5	Absorbance at Wavelength of 254 nm (A ₂₅₄) and Dissolved Organic Carbon (DOC).....	45
3.5.6	Analysis of scavenger.....	47
Chapter 4	Results and Discussions.....	49
4.1	The characteristic of Te-Chi Reservoir.....	49
4.1.1	Water quality of Te-Chi Reservoir.....	49
4.1.2	The organic fractions ratio in NOMs of Te-Chi Reservoir....	52
4.2	Characterization of the assembled catalysts.....	56
4.3	Catalytic ozonation of raw water.....	61
4.3.1	Effect of dosage.....	61
4.3.2	Effect of pH.....	63
4.3.3	The k _d value of catalytic ozonation under first-order reaction.....	65
4.3.4	Catalytic ozonation of coumarin in different pH conditions..	67
4.4	The reduction of THMFPS.....	70
4.5	Modeling catalyst reaction.....	71
4.6	Reuse the catalyst.....	74
Chapter 5	Conclusions and Suggestions.....	76
5.1	Conclusions.....	76

5.2	Suggestions.....	78
	References.....	79



Table List

Table 2.1	Detailed hydrophilic groups and hydrophobic groups of NOMs containing acid, neutrals and bases matters.....	7
Table 2.2	The classification of advanced oxidation processes.....	11
Table 2.3	Homogeneous catalytic ozonation.....	16
Table 2.4	The metal oxide on the support of the ozone decomposition rate.....	21
Table 3.1	Summary of reagents and equipment's for NOMs separation by DAX-8 resin extraction process.....	32
Table 3.2	Reagents and equipment's for preparation of catalyst ($\text{Fe}_3\text{O}_4/\text{SiO}_2/\text{Pd-Mn}$).....	36
Table 3.3	The experimental and online monitor equipment of ozonation system.....	38
Table 3.4	Experimental instruments.....	39
Table 3.5	Basic water quality analysis items and methods.....	40
Table 3.6	Summary of the reagents and equipment used for THMs analysis.....	42
Table 3.7	Analysis instruments of the catalyst ($\text{Fe}_3\text{O}_4/\text{SiO}_2/\text{Pd-Mn}$)....	44
Table 3.8	The instrument and reagent for analysis of NOMs.....	45
Table 3.9	The instrument and reagent of analysis of hydroxyl radicals scavengers.....	48
Table 4.1	The water quality parameters of Te-Chi Reservoir raw water in recent years.....	51
Table 4.2	The percentage distribution of Te-Chi Reservoir NOMs (% of DOC) in recent years (2006-2010).....	55
Table 4.3	The comparison of magnetic particles in different references.....	60
Table 4.4	The comparison of coumarin removal rates (k) for Co, Ag and Pd-Mn catalyst under ozonation.....	70
Table 4.5	Reusability of $\text{Fe}_3\text{O}_4/\text{SiO}_2/\text{Pd-Mn}$ to decompose NOMs under ozonation.....	75

Figure List

Figure 1.1	The algae blooming in Te-Chi reservoir.....	3
Figure 2.1	Schematic of humic acid molecular structure.....	8
Figure 2.2	Schematic of fulvic acid molecular structure.....	8
Figure 2.3	The two type reactions (direct-O ₃ and Radical-type reactions) of ozone in aqueous solution.....	13
Figure 2.4	Mechanisms of catalytic ozonation in the presence of metals on supports.....	19
Figure 2.5	The curve of O ₃ conversion of the catalysts calcined at different temperatures.....	23
Figure 2.6	Formation of 7-hydroxycoumarin (7-HC) in the reaction of coumarin (COU) with hydroxyl radicals.....	24
Figure 3.1	The overall experimental flow chart of this study.....	26
Figure 3.2	The sampling location of Te-Chi Reservoir contain site A, B and C in this study.....	27
Figure 3.3	The flowchart of fractionating five NOMs contents (HAs, FAs, HPOB, HPON and HPI-F) from Te-Chi raw water by DAX-8 resin separation process.....	33
Figure 3.4	Schematic diagrams of ozonation equipment.....	37
Figure 4.1	The percentage of five (HAs, FAs, HPO-N, HPO-B and HPI-F) of organic fraction extracted from Te-Chi reservoir raw water in 2013.....	53
Figure 4.2	SEM image of synthesis of particle calcined in 350°C (a) Pd- activated MnCO ₃ in water (b) Pd- activated MnCO ₃ in ethanol.....	57
Figure 4.3	XRD spectra of Fe ₃ O ₄ /SiO ₂ /Pd-Mn.....	58
Figure 4.4	The zeta potential values of Fe ₃ O ₄ /SiO ₂ /Pd-Mn (pH 3, 5, 7, 9 and 11) and with pHPZC of 10.9.....	58
Figure 4.5	The magnet attracts the catalysts in solution.....	59
Figure 4.6	Field-dependent magnetization hysteresis of Fe ₃ O ₄ /SiO ₂ /Pd-Mn at 25°C.....	59

Figure 4.7	The decomposition of $A_{254 t}/A_{254 0}$ in different catalyst dosage.....	62
Figure 4.8	The mineralization of DOC_t/DOC_0 in different catalyst dosage.....	62
Figure 4.9	The decomposition of rate $A_{254 t}/A_{254 0}$ in different pHs.....	64
Figure 4.10	The mineralization of rate DOC_t/DOC_0 in different pHs.....	64
Figure 4.11	The k_d value of catalytic ozonation in different dosage.....	66
Figure 4.12	The k_d value of catalytic ozonation in different pHs under first-order reaction (based upon DOC).....	66
Figure 4.13	The coumarin removal in the catalytic ozonation under various pHs.....	68
Figure 4.14	The k value of coumarin self-decomposition in different pH (3, 5, 7, 9 and 11) under first-order reaction.....	69
Figure 4.15	The byproduct 7-coumarin in the catalytic ozonation under various pHs.....	69
Figure 4.16	The reduction of THMFPs by sole ozonation and catalytic ozonation ($Fe_3O_4/SiO_2/Pd-Mn$).....	71
Figure 4.17	The Nernst model simulation of A_{254} profiles of catalyst ozonation of Te-Chi Reservoir raw water.....	73
Figure 4.18	The Nernst model simulation of THMFPs profiles of catalyst ozonation of Te-Chi Reservoir raw water.....	74

Nomenclature

NOMs	Natural Organic Matters	天然有機物質
HA	Humic Acid	腐植酸
FA	Fulvic Acid	黃酸
DBP	Disinfection By Products	消毒副產物
THMs	Trihalomethanes	三鹵甲烷
HAAs	Haloaceticacids	鹵化乙酸
HPO-F	Hydrophobic fraction	疏水性成分
HPO-N	Hydrophobic neutrals	疏水性中性物質
HPO-B	Hydrophobic bases	疏水性鹼性物質
HPI-F	Hydrophilic fraction	親水性成分
THMFP	Trihalomethane Formation Potential	三鹵甲烷生成潛能
$\cdot\text{OH}$	Hydroxyl Radicals	氫氧自由基
Pd	palladium	鈰
Mn	manganese	錳
DOC	Dissolved Organic Carbon	溶解性有機碳
HR-SEM	High Resolution Scanning Electron Microscope	高解析掃描式電子顯微鏡

XRD	X-Ray Diffraction	X-光粉末繞射儀
EDS	Energy Dispersive Spectrometer	能量散佈分析儀
pzc	Point of zero charge	零電荷點
TOC	Total Organic Carbon	總有機碳
SQUID	Superconducting Quantum Interference Device	超導量子干涉磁量儀
A ₂₅₄	Absorbance of 254 nm	254nm 波長之吸光度
HPLC	High Performance Liquid Chromatography	高效液相層析儀
O ₃	Ozone	臭氧
ORP	Oxidation Reduction Potential	氧化還原電位
DO	Dissolved	溶氧
k _d	first-order removal rate constant	一階反應速率常數(降解天然有機物)
k	first-order removal rate constant	一階反應速率常數(降解 Coumarin)
COU	Coumarin	香豆素

Chapter 1 Introduction

1.1 Research Background

In Taiwan, most of the sources of drinking water come from the artificial Reservoirs. The Te-Chi reservoir is the storage of the drinking water for the greater metropolitan Taichung region, while it provided power generation as well instance. In recent years, the Te-Chi Reservoir upstream near mountain is planted fruits and vegetable. The farmers used organic fertilizer which would be flown into the reservoir. The natural organic matters (NOMs) cause eutrophication and polluted the water quality. NOMs consist of two parts: humic substances (HS), which are composed of fulvic acids (FAs), humic acids (HAs) and non-humic substances (non-HS), which include carbohydrates, lipids, and amino acids (Karnik *et al.*, 2005). In general, the non-HS fraction of the NOMs may generally more biodegradable and, as such, it supports bacterial regrowth in water distribution systems (Zazouli *et al.*, 2008; Bougeard *et al.*, 2010). Humic acid is during the chlorination disinfection process of water which would be produce disinfection by-products (DBPs) such as trihalomethanes (THMs) and haloacetic

acid (HAAs) (Matilainen *et al.*, 2011; Adams *et al.*, 2014). The DBPs caused the risk of cancer for human health (Zularisam *et al.*, 2006). Therefore, degradation DBPs in water treatment process has become an important issue.

The conventional water treatment can't effectively remove the DBPs, so the advanced oxidation processes (AOPs) would be used as a powerful oxidizing method to removal DBPs. The AOPs usually degrade organic of pollution in the water treatment. AOPs comprise alone O₃, UV/O₃, electrochemical oxidation, Fenton, photo-Fonton, wet oxidation, sono-catalytic ozonation, catalytic ozonation etc. AOPs generate act as a strong oxidant hydroxy radicals transform pollution (Rupa *et al.*, 2011). The •OH radical is an extraordinarily reactive species; it attacks most part of organic molecules (Li *et al.*, 2009). Catalytic ozonation used a solid catalyst has been the issue of increasing levels of interest from the drinking water and wastewater treatment industries (Li *et al.*, 2014). It is not completely clear whether catalysts cause ozone decomposition leading to the formation of hydroxyl radicals and that the presence of metal oxides accelerates the generation of hydroxyl radicals during ozonation (Rosal *et al.*, 2010).

The catalytic activity order of metals supported on SiO₂ was found to be: Pd > Ag > Rh > Pt > Ni > Ru. Among all these, because of the ease of recovery and separation, modified magnetic particles have been used for catalytic ozonation in recent years (Lin *et al.*, 2012). In this study, Pd-Mn has been selected as the catalyst in ozonation system for decomposing retardant humic acid in raw water and investigated the mechanism in different conditions.



Figure 1.1 The algae blooming in Te-Chi reservoir (2013).

1.2 Objectives

The objectives of this study are:

1. Comparing the basic water quality, the composition of natural organic matter in Te-Chi Reservoir.
2. Synthesizing magnetic metal nanoparticle catalyst ($\text{Fe}_3\text{O}_4/\text{SiO}_2/\text{Pd-Mn}$).
3. Degrading of natural organic matters (NOMs).
4. Reducing hazardous DBPs generated from NOMs.
5. Investigating the mechanisms of hydroxyl radical in the catalytic ozonation.

Chapter 2 Literature Review

2.1 Natural Organic Matters (NOMs) in water

Natural organic matters (NOMs) is a foremost concern in drinking water treatment since it causes confrontational water qualities such as color, taste and odour (Baghoth *et al.*, 2011). Natural organic matters (NOMs) produced through the decomposition of plants, animal residues and human activities or environmental microbial degradation result in the formation complex mixture organic matter in fresh surface water (Valencia *et al.*, 2014; Matilainena *et al.*, 2011). NOMs have different kinds of organic matter due to variety of environments that containing three major portions ,which are hydrophobic fraction (HPO-F) or operationally defined as humic fraction with mainly carboxylic and phenolic functional groups(humic acids (HA) and fulvic acids), transphilic fraction (TPI), which has lower aliphatic/aromatic carbon contents than the HPO-B, and hydrophilic fraction(HPI-F) or non-humic fraction corresponding to bases (primary and secondary protein groups), acids(amino acids), and neutral HPI-F (polysaccharide groups) (Zularisam *et al.*, 2011). Table 2.1 shown detailed hydrophobic and

hydrophilic groups of the NOMs. HAs, aliphatic amines, tannins and aliphatic carboxylic acids are part of hydrophobic group, which contains low to moderate molecular weight whereas the hydrophilic group comprises low molecular weight carbohydrates, proteins and amino acids. The humic substances (HSs) of NOMs are divided into two kinds: humic acid (HA) and fulvic acid (FA). Humic and fulvic acids are difficult to be biodegradable, due to its complex organic molecules, including peat and soil organic matter content about 60-80%. Bacterial and chemical degradation of lignin and other plant structural carbohydrates is responsible for the formation of humic acid, fulvic acid and intermediate products (Zularisam *et al.*, 2006). The HAs and the FAs are anionic polyelectrolyte with negatively charged carboxylic acid (-COOH), methoxyl carbonyls (C=O) and phenolic (-OH) functional groups. Figures 2.1 and 2.2 are shown models of HA and FA molecular structures (Stevenson, 1982; Buffle, 1997; Zularisam *et al.*, 2011). Humic acid (HA) is the fraction soluble in an alkaline solution, fulvic acid (FA) is the fraction soluble in an aqueous solution regardless of pH, and humin is the fraction insoluble at any pH value (Badis *et al.*, 2010).

Table 2.1 Detailed hydrophilic groups and hydrophobic groups of NOMs containing acid, neutrals and bases matters.

	Acid	Neutral	Base
Hydrophilic groups (HIP)	Aliphatic acids of less than five carbons, Hydroxyl acids, Sugars, Low molecular weight alkyl mono carboxylic and dicarboxylic acids.	Aliphatic amines less than nine carbons, Amino acids, Pyridines, Purines, Pyrimidines, Low molecular weight alkyl amines.	Aliphatic amides, Alcohols, Aldehydes, Esters, Ketones with less than five carbons, and Polysaccharides.
Hydrophobic groups (HOP)	Aliphatic carboxylic acids of five to nine carbons, One and Two-ring aromatic carboxylic acids, Aromatic acids, One and Two-ring Phenols, and Tannins.	Aliphatic alcohols, Alkyl alcohols, Ethers, Ketones, and Aldehydes, Aliphatic carboxylic acids and Aliphatic amines with more than five carbons, Aromatic carboxylic acids with more than nine carbons, and Aromatic amines of three rings and greater.	Proteins, One and Two-ring aromatic amines except Pyridine, and High molecular weight alkyl.

(Marhaba *et al.*, 2006)

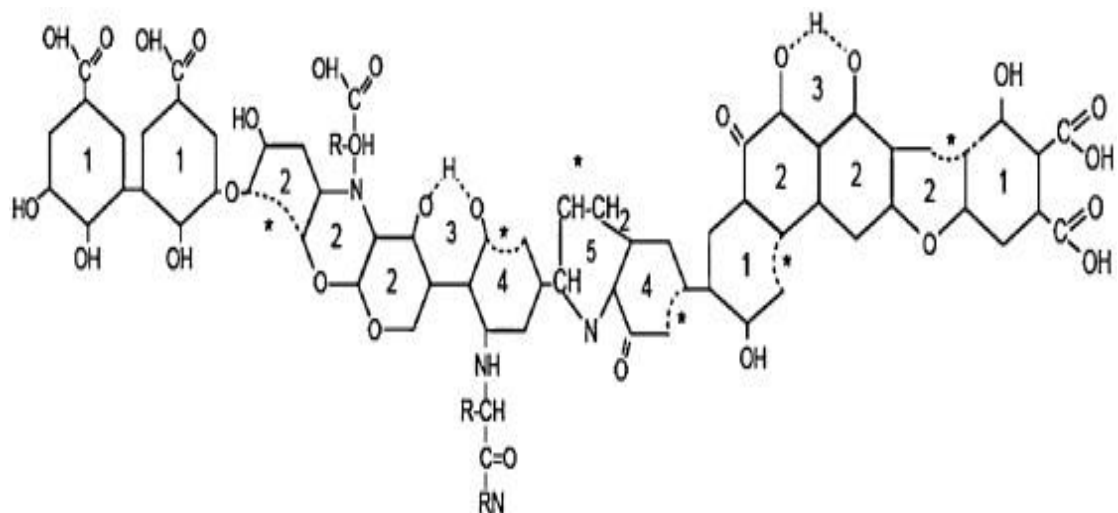


Figure 2.1 Schematic of humic acid molecular structure (Stevenson, 1982; Zularisam *et al.*, 2011).

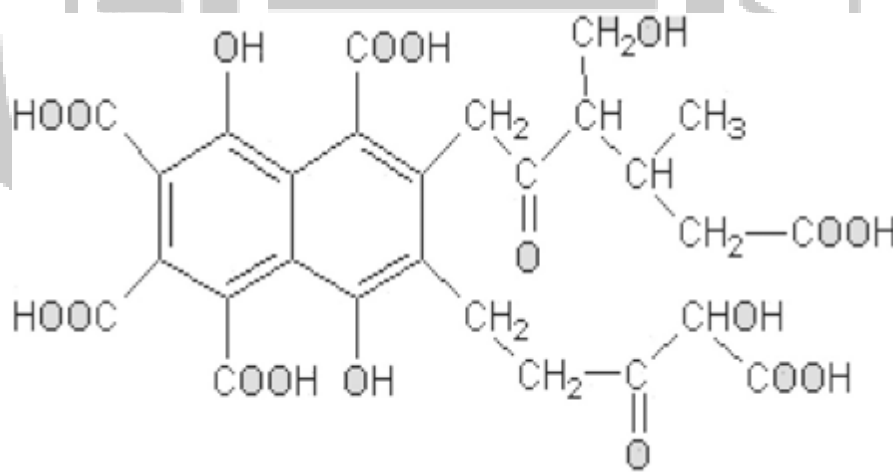


Figure 2.2 Schematic of fulvic acid molecular structure (Buffle, 1997).

2.2 Disinfection by-products (DBPs)

The chlorine disinfection was commonly used in drinking water treatments, which have low cost, excellent bactericidal capacity, high oxidizing potential and persistent disinfection (Jones *et al.*, 2012). Several studies reactions between natural organic matter (NOM) and chlorine form different types of disinfection byproducts (DBPs) in drinking water. DBPs contain trihalomethanes (THMs), haloacetic acids (HAAs), haloacetonitriles (HANs), haloketones (HKs), nitrosamines and other known and unknown byproducts (Chowdhury *et al.*, 2011; Liu *et al.*, 2011). These DBPs can be associated with human bladder cancer and other chronic and sub-chronic effects on human health (Chowdhury *et al.*, 2011; Zularisam *et al.*, 2006). United States Environmental Protection Agency (USEPA, 2009) set up a control criterion for concentration of THMs in drinking water (0.08 mg/L). In order to the generation of DBPs are decreased, the best way is to remove the precursor of NOMs before chlorination.

2.3 Advanced Oxidation Processes (AOPs)

Advanced oxidation processes (AOPs) are new water treatment technology in the past several years that are mainly used to treat polluted underground water, drinking water, industrial water and retardant substance. AOPs contain the combined use of ozone with hydrogen peroxide and/or UV radiation; hydrogen peroxide with ferrous iron addition, and others (Rosenfeldt *et al.*, 2006; Lau *et al.*, 2007; Valdes *et al.*, 2009; Ikhlaiq *et al.*, 2012). The classification of AOPs is shown in Table 2.2. These are based on the enhanced transformation of ozone into $\cdot\text{OH}$ radicals which have a high reactivity with most inorganic and organic micropollutants (Acero and von Gunten, 2001).

Table 2.2 The classification of advanced oxidation processes.*

Reaction classification	Advanced oxidation processes
Homogeneous systems without irradiation	O_3/H_2O_2 , O_3/OH^- , H_2O_2/Fe^{2+} (Fenton's reagent)
Homogeneous systems with irradiation	O_3/UV , H_2O_2/UV , $O_3/H_2O_2/UV$, photo-Fenton, electron beam, ultrasound, vacuum-UV
Heterogeneous systems with irradiation	$TiO_2/O_2/UV$
Heterogeneous systems without irradiation	Electro-Fenton.

*(Kasprzyk-Hordern *et al.*, 2003)

2.3.1 Ozone reaction

Ozone is a powerful oxidant that can degrade organic pollutants in water. It reacts quickly with organic compounds containing unsaturated bonds and amino groups (Ikhlaq *et al.*, 2012). In addition to direct oxidation, ozone decomposes via a chain indirect reaction mechanism to form $\cdot\text{OH}$ radicals, which in turn can oxidize the pollutant (Hoigne, 1982).

The mechanism of ozone and organic reaction can be divided into the direct and indirect reactions, while the oxidation mechanism of the direct reaction and indirect reaction may occur simultaneously. Two types of ozone reactions in aqueous solution are shown in Figure 2.3. In the direct reaction, ozone selectively attacks the unsaturated electron-rich bonds and easily reacts with specific functional groups, such as aromatics, olefins and amines ($10^{-7}\sim 10^7 \text{ M}^{-1}\text{S}^{-1}$) (Chang, 2010). In the indirect oxidation, the ozone decomposes via a chain reaction mechanism to form $\cdot\text{OH}$, which has a higher oxidation potential than ozone. In the indirect oxidation, the ozone decomposes via a chain reaction mechanism to form $\cdot\text{OH}$, which has a higher oxidation

potential more than ozone. The reaction rate of $\cdot\text{OH}$ is fast and low selectivity ($10^7 \sim 10^{10} \text{ M}^{-1} \text{ S}^{-1}$) (Van Gunten, 2003).

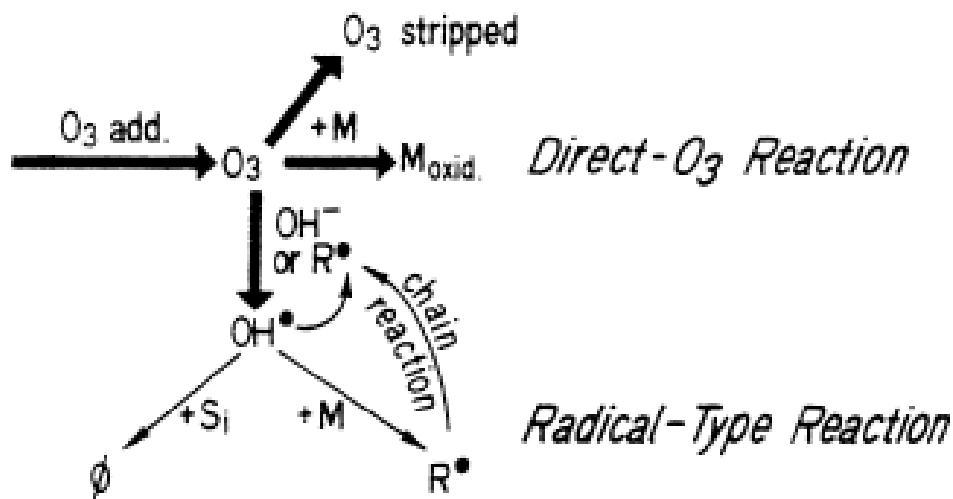


Figure 2.3 The two type reactions (direct- O_3 and Radical-type reactions) of ozone in aqueous solution (Langlais *et al.*, 1991).

M: Solute

S_i : The free radicals scavenge

R: The radical catalyzed by decomposition of ozone

M_{oxid} : Solute oxidized

\emptyset : The oxidized product that can't be decomposed by ozone

2.3.2 Catalytic ozonation

Ozone is a selective oxidant, it preferentially attacks molecules containing unsaturated bonds, leading to the formation of saturated compounds such as aldehydes, ketones and carboxylic acids (Lin, 2012) therefore, sole ozonation is not sufficient for mineralization of pollutants. To overcome this problem, the combination of ozone with catalysts increases the decomposition of ozone to form $\cdot\text{OH}$ in order to achieve the mineralization or improve ozone reaction with several organic compounds has been investigated (Rosal *et al.*, 2008). Catalysis combined with the ozonation processes (catalytic ozonation) can improve the oxidation and degradation of organic contaminant compounds (Liotta *et al.*, 2009). Catalytic ozonation includes both homogeneous and heterogeneous catalytic ozonation.

2.3.2.1 Homogeneous catalytic ozonation

Homogeneous catalytic ozonation is the use transition metal ions decomposition with ozone. Two major mechanisms of homogeneous catalytic ozonation:

1. Decomposition of ozone by metal ions leading to the generation of free radicals (Skoumal *et al.*, 2001).
2. Complexes formation between organic matters and the catalyst and consecutive oxidation of the complex (Beltrán *et al.*, 2005).

Several metal ions were found to be effective as catalysts of the ozonation process. Among them widely used are: Mn(II), Fe(III), Fe(II), Co(II), Cu(II), Zn(II) and Cr(III). Fe (II)/O₃ and Fe (II)/O₃/UV processes are based on Fenton or photo-Fenton reactions.

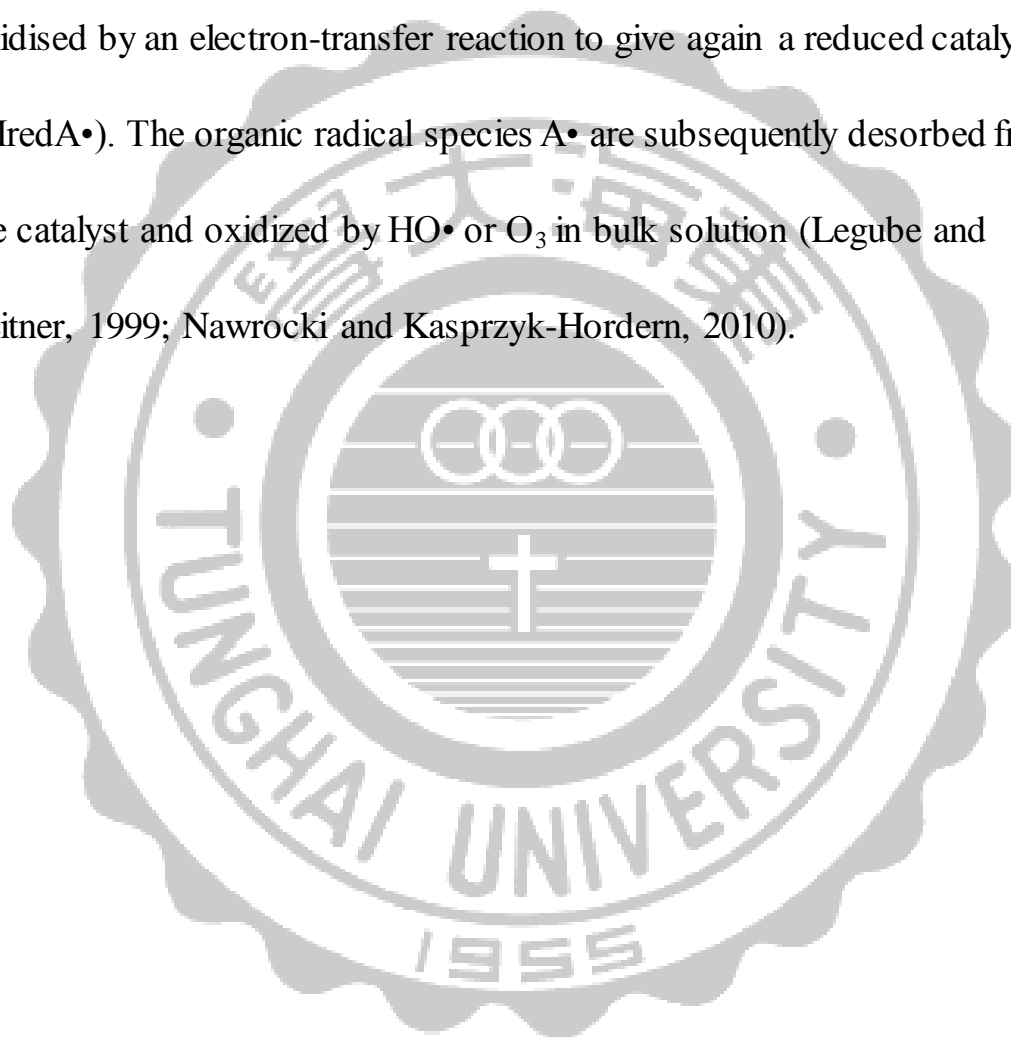
Table 2.3 Homogeneous catalytic ozonation.

Catalyst	Organic compound	Reference
Fe(II), Cu(II), Ni(II), V(V), Mo(VI),	Dinitrobenzene (DNB)	Trapido <i>et al.</i> , 2005
Mn(II), Fe(II), Fe(III)	Chlorobenzenes	Cortes <i>et al.</i> , 2000
Ni(II), Fe(II), Mn(II), Zn(II), Sr(II), Cr(III), Cd(II), Hg(II), Cu(II)	1,3,6-Naphthalenetrisul- fonic acid	Sánchez-Polo and Rivera-Utrilla, 2004
Mn(II), Fe(II), Fe(III), Cr(III), Ag(I), Cu(II), Zn(II), Co(II), Cd(II)	Humic substances	Gracia <i>et al.</i> , 2000
Ce(III)	Phenol	Matheswaran <i>et al.</i> , 2007
Co(II)	Oxalic acid, pyruvic acid	Carbajo <i>et al.</i> , 2006
Fe(II), Fe(III), Mn(II), Co(II)	Lignin sulfonate	Ksenofontova <i>et al.</i> , 2003
Fe(III)	Oxalic acid	Beltrán <i>et al.</i> , 2005
Mn(II), Fe(II), Fe(III), Zn(II), Co(II), Ni(II)	Azo dyes	Wu <i>et al.</i> , 2008

2.3.2.2 Heterogeneous catalytic ozonation

Heterogeneous catalytic ozonation aims to enhance the removal of highly refractory compounds by the transformation of ozone into more reactive species and/or by adsorption and reaction of the pollutants on the surface of the catalyst (Liotta *et al.*, 2009). Heterogeneous ozonation using a solid catalyst has been the subject of increasing levels of interest from the drinking water and wastewater treatment industries. There are several key advantages to this technology, including its ability to (1) enhance the reaction rate of the sole ozonation process; (2) improve the mineralization process; and (3) reduce the yield of the intermediates and the toxicity of the effluent. A variety of different catalysts are commonly used for this process, including activated carbon, minerals, molecular sieves, transition metal oxides and supported metal/metal oxides (Zhao *et al.*, 2013). Figure 2.4 show the mechanisms of catalytic ozonation in the presence of metals on supports. In the first mechanism organics adsorb on the surface of the catalyst and are attacked by ozone (or hydroxyl radicals) from bulk solution to give oxidation products.

In the second mechanism, both ozone and organic molecules adsorb on the surface of the catalyst. On the surface of reduced Me-catalyst (M_{red}) ozone oxidises metal with the generation of OH radicals. Organic molecules (AH) after adsorption on the catalyst surface are subsequently oxidised by an electron-transfer reaction to give again a reduced catalyst ($M_{red}A^\bullet$). The organic radical species A^\bullet are subsequently desorbed from the catalyst and oxidized by HO^\bullet or O_3 in bulk solution (Legube and Leitner, 1999; Nawrocki and Kasprzyk-Hordern, 2010).



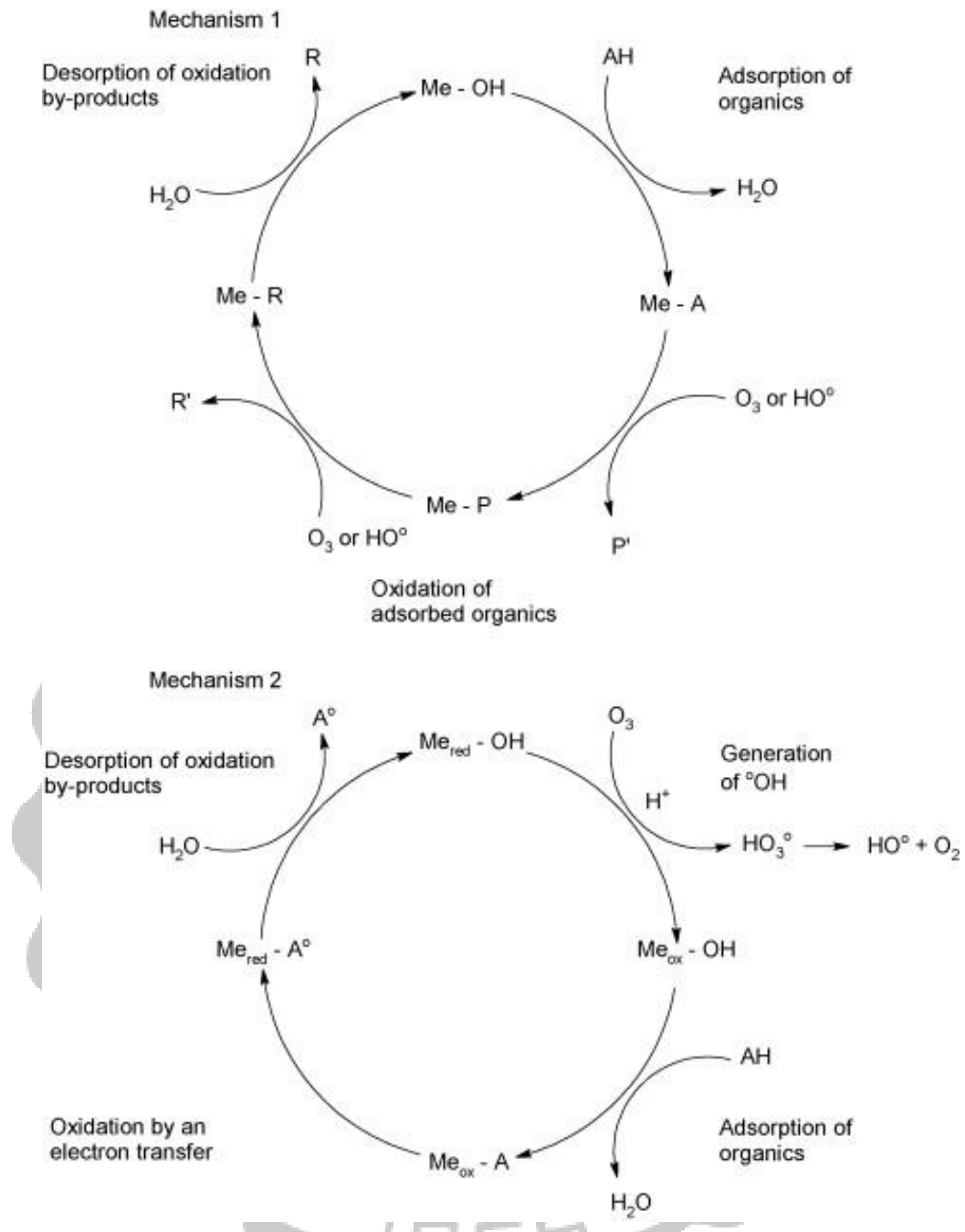


Figure 2.4 Mechanisms of catalytic ozonation in the presence of metals on supports (AH: organic acid; P, R: adsorbed primary and final by-products; P', R': primary and final by-products in solution respectively; modified from) (Nawrocki and Kasprzyk-Hordern, 2010).

2.4 Catalyst

2.4.1 Metal oxide and metal oxide on support

Heterogeneous catalysts commonly are activated carbon, minerals, molecular sieve, transition metal oxides and supported metal/metal oxides (Zhao *et al.*, 2013). Metal oxides represent one of the most important and widely employed classes of solid catalysts, either as active phases or supports. The coated metal on the surface of the solid catalyst have higher ozone decomposition rate, the increase in the frequency of the electron transport and making the redox reaction increased. Manganese oxides are the most widely studied metal oxides as ozonation catalyst, and they are reported to be the most efficient in ozone decomposition (Kasprzyk-Hordern *et al.*, 2003). Manganese salts and oxides have been used as active catalysts in the homogeneous and heterogeneous catalytic ozonation systems and its efficiency has been proved for several organic compounds (Orge *et al.*, 2012). The application of both metal and support of catalysts in noble metals are efficient redox catalysts, which are able to decompose O_2 with the formation of oxygen-metal bound strong enough to provide effective ozone decomposition (Nawrocki and Kasprzyk-Hordern, 2010).

Table 2.4. The metal oxide on the support of the ozone decomposition rate.

(adapted from Kasprzyk-Hordern *et al.*, 2003)

	Al ₂ O ₃	SiO ₂	SiO ₂ -Al ₂ O ₃	TiO ₂
Metal	Average rate (mg _{O3} min ⁻¹ g ⁻¹ cat)			
Ru	0.24	0.18	0.24	0.07
Rh	0.49	0.49	0.27	0.20
Pd	0.40	0.77	0.53	0.36
Ag	0.39	0.56	0.14	0.28
Ni	0.16	0.22	0.07	0.09
Pt	0.24	0.48	0.07	0.26

2.4.2 Nanoparticles and nanocatalysts

Nanoparticles are solid and spherical structures ranging around 100 nm in size and prepared from natural or synthetic polymers. Within this range, the material of the nanostructures will have completely different properties (compared to the original size) because of quantum effects.

Nanoparticles is widely used in catalysts, biomedical (drug delivery, cell stain) and high-tech industries (Lin, 2012). Recently, an increasing number of researchers focused on nanocatalysts which could be

potentially used in the heterogeneous catalytic ozonation. Compared with conventional catalysis, nanocatalysis is able to design catalysts with excellent activity, greater selectivity and high stability. Nanocatalysis characteristics can be obtained by tailoring the size, shape, morphology, composition, electronic structure and thermal and chemical stability of the particular nanomaterials (Polshettiwar *et al.*, 2011).

2.4.3 Pd-Mn catalysts

The catalytic materials selected are usually noble metals like Pd or Pt, or oxides of transition metals such as Mn, Co, Ni and Ag (Heisig *et al.*, 1997; Zhao *et al.*, 2013). Figure 2.5 show the activity of the Pd-Mn catalysts increases with the increasing of reaction temperature. The catalysts in image have the best activity as the calcined temperature is 350 °C.

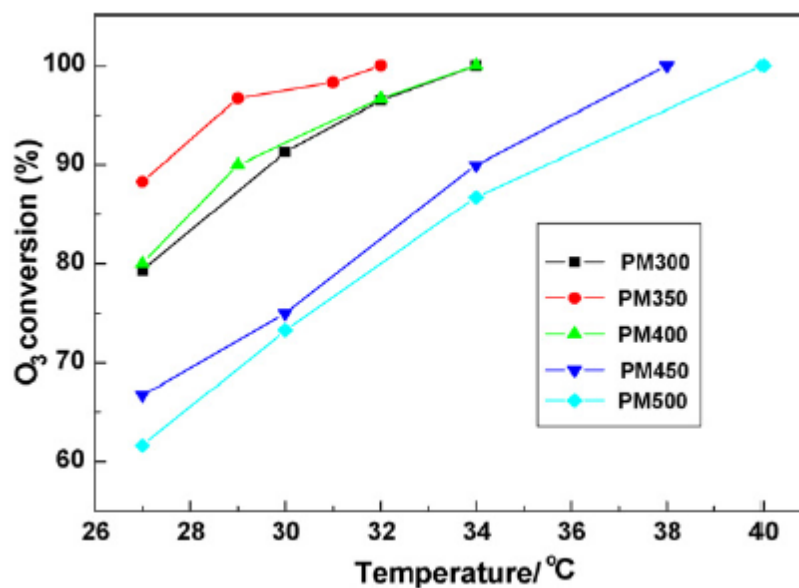


Figure 2.5 The curve of O₃ conversion of the catalysts calcined at different temperatures. PM300: 300 °C; PM350: 350 °C; PM400: 400 °C; PM450: 450 °C; PM500: 500 °C (Yu, *et al.*, 2009).

2.5 Hydroxyl radical scavengers

AOPs could produce oxidants such as the ·OH a much more powerful oxidant than ozone. The ·OH can react non-selectively to oxidize many organic compounds, and it was difficult to measure ·OH because its short lifetime (usually 10⁻⁹ s in a cell) hinders its direct detection. Coumarin (COU) has been used as a probe molecule as it is known to react with hydroxyl radicals leading to the formation of fluorescent 7-hydroxycoumarin (7HC) (Ikhlaiq *et al.*, 2012) (Figure 2.6).

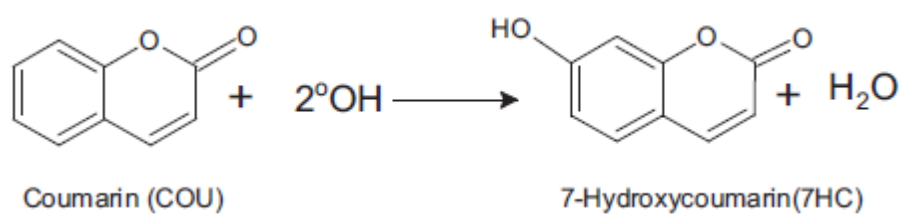


Figure 2.6 Formation of 7-hydroxycoumarin (7-HC) in the reaction of coumarin (COU) with hydroxyl radicals (Ikhlq *et al.*, 2012).



Chapter 3 Material and Methods

3.1 Experiment Frameworks

The purpose of this study was to remove the natural organic matters and investigate the reaction mechanisms in heterogeneous catalytic ozonation processes. The overall experimental flow chart is shown in Figure 3.1. The first part is to understand water quality and the composition of NOMs in Te-Chi Reservoir raw water. Secondly, we synthesized the magnetic nanoparticles ($\text{Fe}_3\text{O}_4/\text{SiO}_2/\text{Pd-Mn}$) and combined with ozonation to decompose NOMs and find out the best operational parameters (dosage and pH). Finally, catalytic ozonation was investigated to elucidate the reaction mechanism.

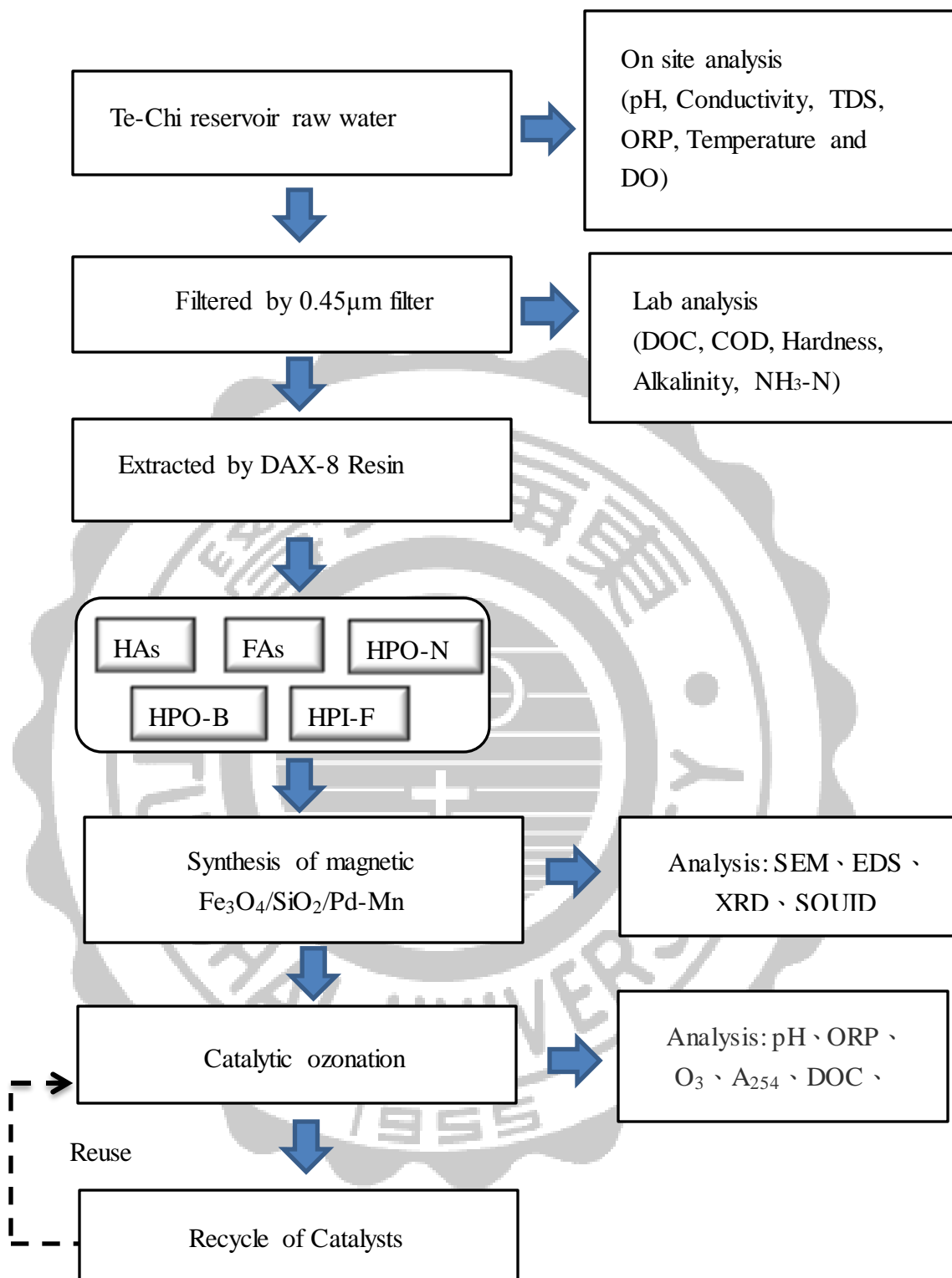


Figure 3.1 The overall experimental flow chart of this study.

3.2 Sample Preparation and Fractionation Procedures

3.2.1 Sampling Site and Preservation

Water samples of this study were collected from Te-Chi Reservoir at Taichung County, Taiwan on August 06, 2013. A total 15 set of 20L polyethylene buckets were full of samples and the buckets were covered by the black plastic bags to prevent the sun radiation during the transportation of raw water. The water samples were preserved at 4°C before analysis. The items analyzed in field were pH, DO, total dissolved solids (TDS), water temperature, and conductivity. The sampling location A, B and C of Te-Chi Reservoir are shown in Figure 3.2.

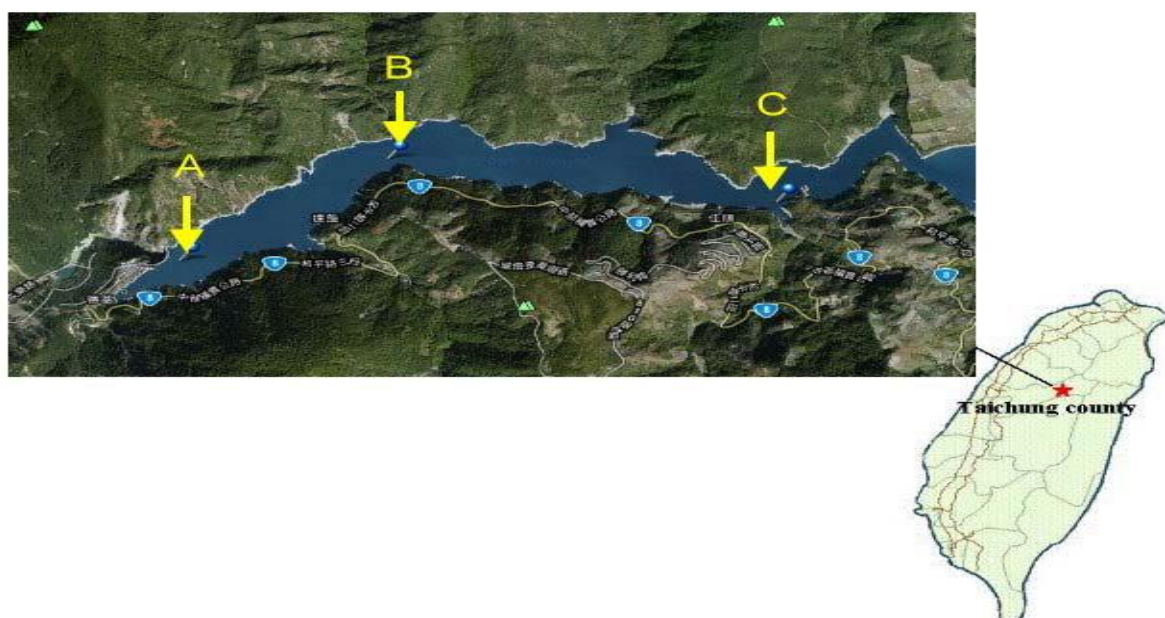


Figure 3.2 The sampling location of Te-Chi Reservoir contain site A, B and C in this study.

3.2.2 Extraction procedure

The pre-treatment steps of DAX-8 resins:

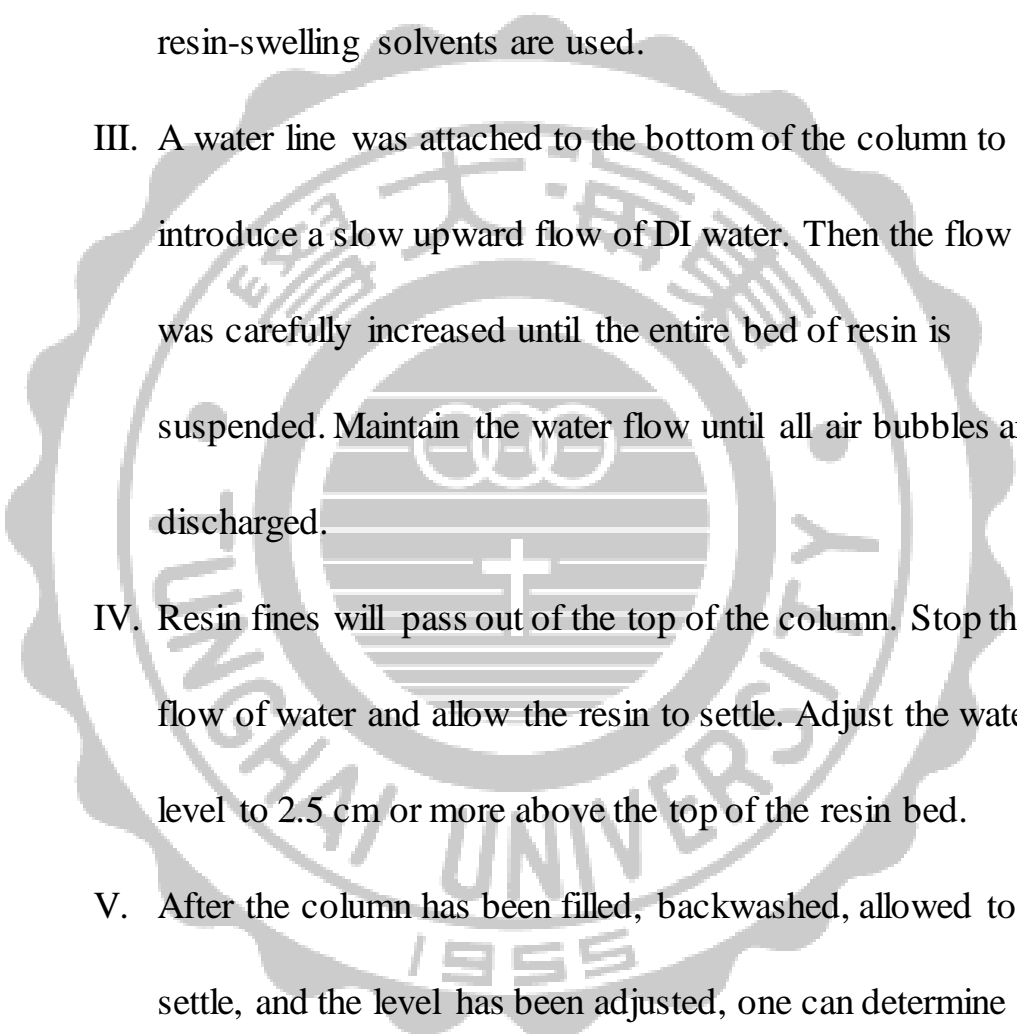
1. Resin Wetting Procedure

- I. Transfer the dry resin to a 500 mL beaker, then add sufficient methanol to cover the resin bed by 2.5-5 cm. Stir the resin gently for a minute to ensure complete mixing.
- II. Allow the resin to stand for 15 minutes carefully decants most of the methanol and replaces it with deionized (DI) water.
- III. Stir the mixture and then allow it to stand for 5-10 minutes.
- IV. Repeat the above steps to remove the residual methanol.

The rinsed water effluent was monitored by TOC analyzer to make sure no methanol residue in DAX-8 resins.

2. Preparation of Resin Columns

- I. Add approximately 2.5 cm of DI water was into the Pyrex glass column (5 cm inside diameter (ID) and 60 cm in length) before adding the resin slurry, then slowly pouring the resin slurry into the column.

- 
- II. As the column fills, drain excess water through the bottom of the column, but do not allow the liquid level to fall below the top of the resin bed. Add enough resin to half-fill the column only. This will allow room for expansion when resin-swelling solvents are used.
- III. A water line was attached to the bottom of the column to introduce a slow upward flow of DI water. Then the flow was carefully increased until the entire bed of resin is suspended. Maintain the water flow until all air bubbles are discharged.
- IV. Resin fines will pass out of the top of the column. Stop the flow of water and allow the resin to settle. Adjust the water level to 2.5 cm or more above the top of the resin bed.
- V. After the column has been filled, backwashed, allowed to settle, and the level has been adjusted, one can determine the volume of resin in the column by Eq. 3.1

$$V = \pi \times (1/2 \times ID)^2 \times L \dots \dots \dots \text{Eq. 3.1}$$

V: volume of a cylinder.

ID: inside diameter.

L: length of the bed.

The isolation procedures utilized the raw water through the column allow compounds of interest to adsorb to the resin. Adsorption is an equilibrium phenomenon, and the most effective flow rate for loading the resin is within the range of 2-16 bed volumes per hour. Flow rates at the lower end of the range allow higher adsorb rate through the adsorbent bed.

At first, the 90 L raw water sample was filtered through a 0.45 μm cellulose acetate filter paper (ADVANTEC®, Japan) to remove the suspended solids then the pH value was adjusted to 13 by adding 2N HCl and 2N NaOH.

After that, the filtered water was passed through the first DAX-8 resins column at a flow rate of 25 mL/min followed by eluting with 20 L 0.1N HCl to recover the HPOB, which was adsorbed on the resins.

The pH of the effluent was adjusted to 7 with 2N HCl or 2N NaOH.

The second solution was then introduced into a second DAX-8 resins column at the same flow rate of 25 mL/min. The remaining DAX-8 resin in the second column was to move Soxhlet extractor, dried at 60 °C and eluted with methanol to collect HPON. A vacuum instrument combined with high-purity nitrogen gas (99.99 %) was used to evaporate the methanol solution. The concentrated HPON was dissolved in 500 mL DI water as a stock solution.

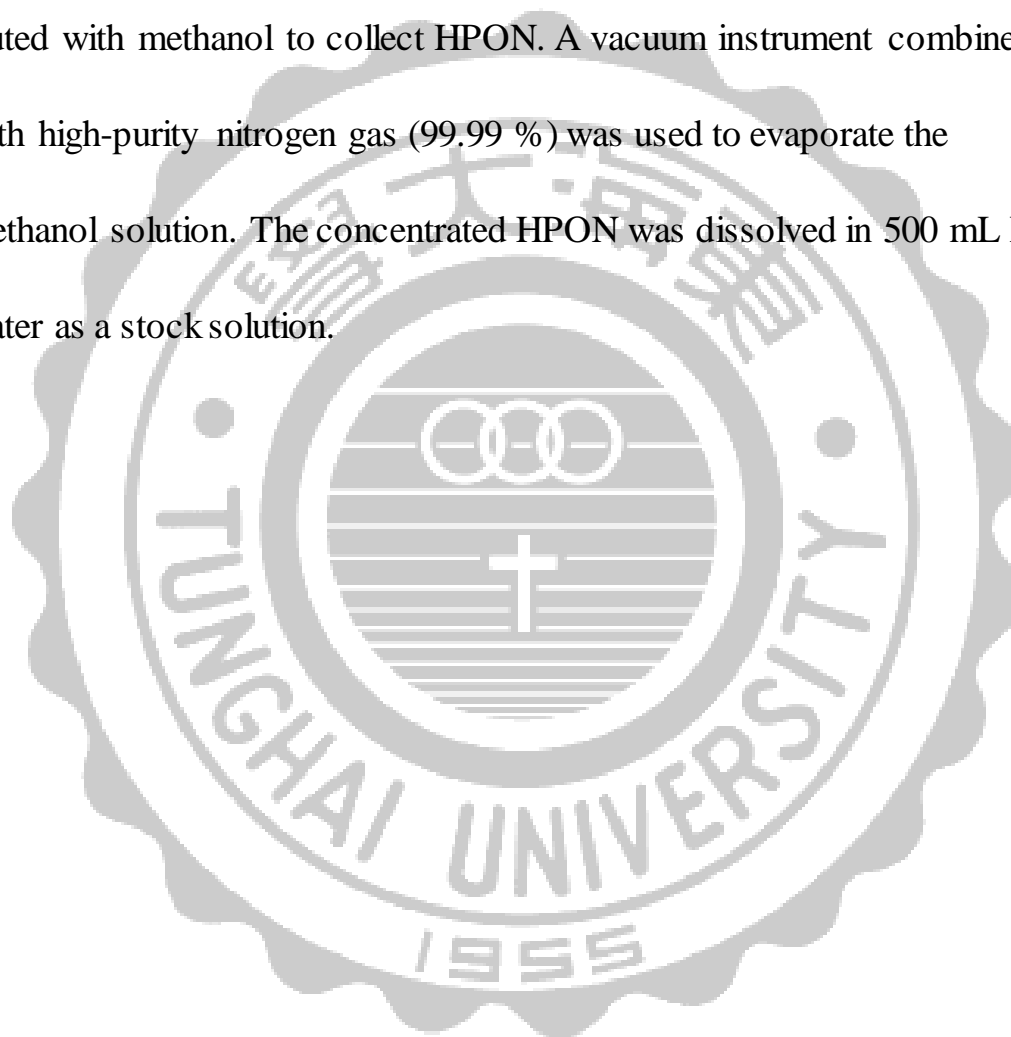


Table 3.1 Summary of reagents and equipment's for NOMs separation by DAX-8 resin extraction process.

Equipment	Series Number, Maker, Country
DAX-8 resins	Supelite DAX-8, Supelco, a new substitute for XAD-8
Glass column	Pyrex 5 cm, inside diameter × 60 cm, local supply
Teflon tubing	Made in Japan
Peristalsis pump	Peristaltic pump System Model No. 7553-80, Cole-Parmer, USA
Soxhlet extractions	Pyrex, local supply
Vacuum instrument	EYELA, Aspirator A-3S, RTE-100LP
Reagent	Cas/Catalog/HS number, Maker, Country
HCl	2806-10-00, Merck, Germany
NaOH	1310-73-2, Merck, Germany
Hexane	110-54-3, Merck, Germany
Acetonitrile	75-05-8, Merck, Germany
Methanol	67-56-1, Merck, Germany

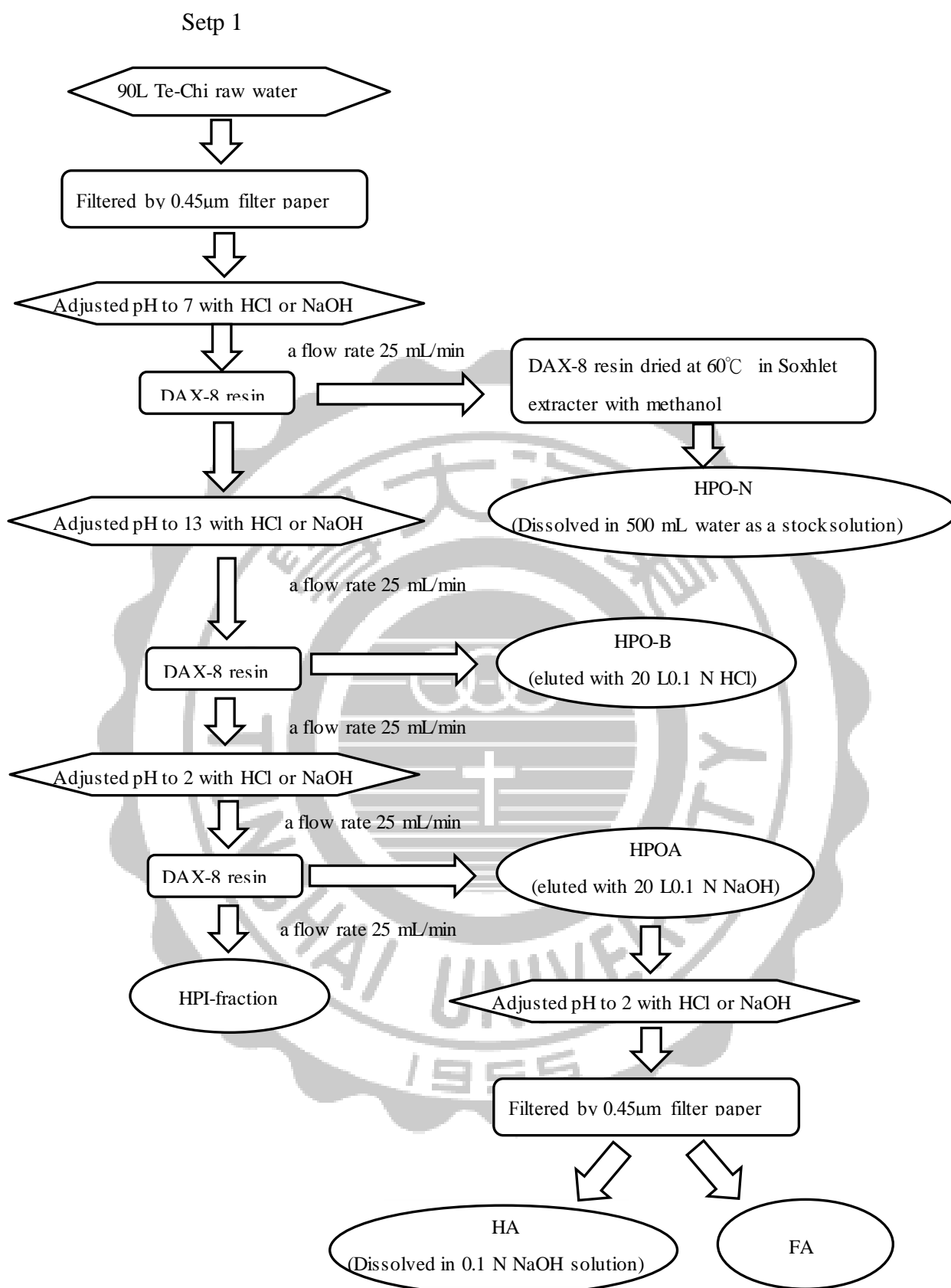


Figure 3.3 The flowchart of fractionating five NOMs contents (HAs, FAs, HPOB, HPON and HPI-F) from Te-Chi raw water by DAX-8 resin separation process.

3.3 Preparation of catalyst

3.3.1 Synthesis of Fe_3O_4 :

The catalysts used in this study were self-synthesized magnetic palladium-manganese ($\text{Fe}_3\text{O}_4/\text{SiO}_2/\text{Pd-Mn}$) and all the reagents were supplied by Merck Chemical Ltd. Fe_3O_4 was the core of the particles with magnetic was obtained by co-precipitation (Mahmoodi and Mohammad, 2011). Briefly, ferric chloride ($\text{FeCl}_2 \cdot 4\text{H}_2\text{O}$) and ferrous chloride (FeCl_3) were added to deionized water at 75°C . Then added to ammonia hydroxide (NaOH) deionized water while solution was heated to 85°C . After the completely mixed, the black precipitates (Fe_3O_4) were separated by magnetic and washed three times with deionized water.

3.3.2 Synthesis of $\text{Fe}_3\text{O}_4/\text{SiO}_2$:

$\text{Fe}_3\text{O}_4/\text{SiO}_2$ structures were prepared by sol-gel method (Ghosh *et al.*, 2011). Fe_3O_4 particles mix deionized water, ammonia hydroxide and added solvent (deionized water, ammonia and isopropanol) then the solution shaken 30 minutes by ultrasound. After that, tetraethyl orthosilicate (TEOS) was added to the solution slowly at 40°C and the solution was stirred (550 rpm) for 6 hours. After washed and dried at

110°C,

3.3.3 Synthesis of Fe₃O₄/SiO₂/Pd-Mn:

Fe₃O₄/SiO₂/Pd-Mn was prepared by incipient wetness impregnation method (Guo *et al.*, 2006). Fe₃O₄/SiO₂ mixed active MnCO₃ and Pd(NO₃)₂ • 2H₂O solution. The solution was shaken for 24 hour then dried for 24 hour and calcined (Yu *et al.*, 2009).

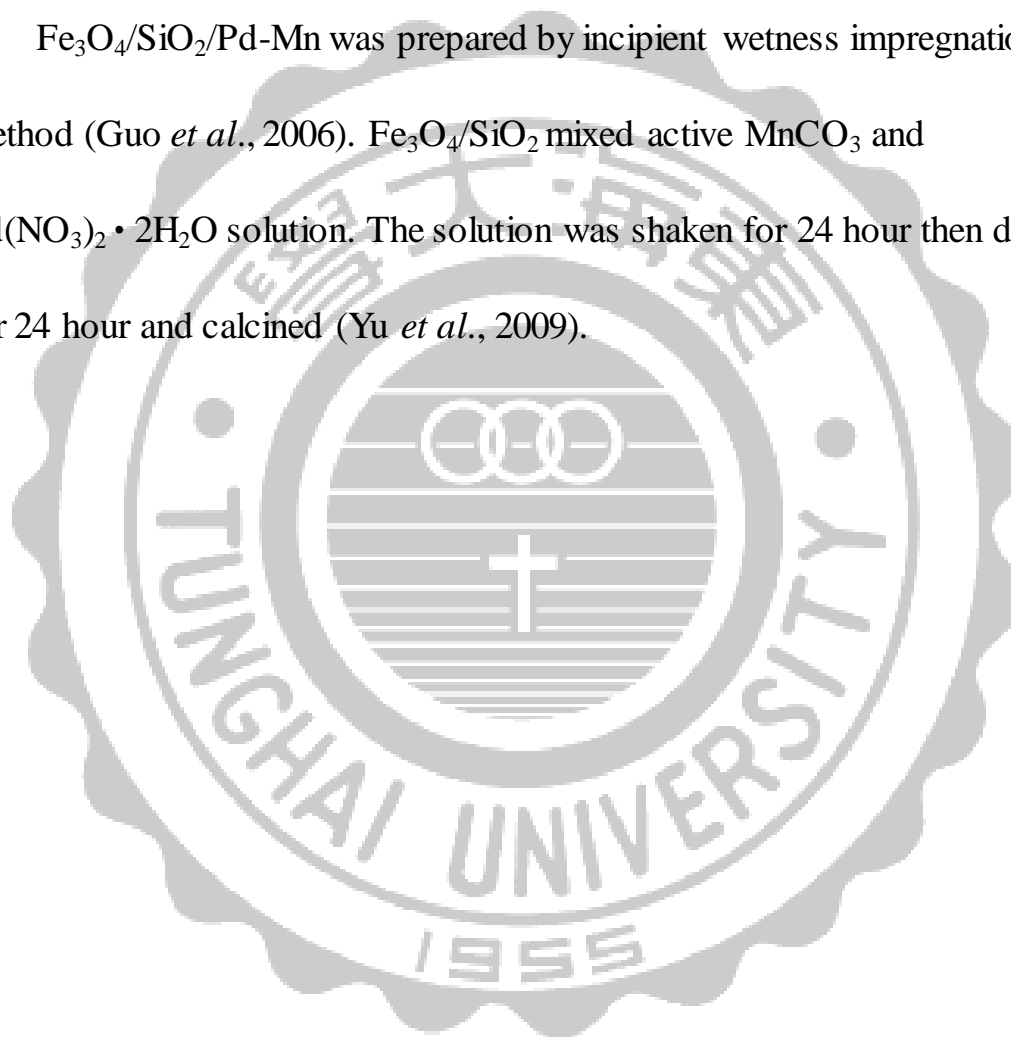


Table 3.2 Regents and equipment's for preparation of catalyst
(Fe₃O₄/SiO₂/Pd-Mn).

Reagent	Cas/Catalog/HS number, Maker, Country
FeCl ₂ *4H ₂ O	13478-10-9, Merck, Germany
FeCl ₃	7705-08-0, Merck, Germany
NH ₄ OH	2814-20-00, Merck, Germany
Isopropanol	67-63-0, Mallinckrodt, USA
Tetraethyl orthosilicate	78-10-4, Merck, Germany
N ₂ O ₆ Pd*2H ₂ O	32916-07-7, Merck, Germany
MnCO ₃	598-62-9, J. T. Baker, USA
C ₂ H ₅ OH	2806-10-00, Osaka 島久藥品, Japan
Equipment's	Model, Maker, Country
Ultrasonic cleaning bath	Power Sonic 420, Hwashin Technology, South Korea

3.4 Ozonation and Catalytic Ozonation System

Figure 3.4 shows the ozonation system, and the gas phase of ozone produced from pure oxygen (AirSep Corp., KA-1600, USA) generation after high voltage discharge, then inflow the glass batch reactor of 3 liter with the agitator speed of 200 rpm (Shin kwang, DC-1S, Taiwan) under water bath controlled at $25\pm 2^{\circ}\text{C}$. Three online monitored sensors (pH, ORP and DO_3) (Suntex, TS1, Taiwan) connected with oscilloscope (Yokogawa, OR100E, Japan) recorder were used in this study.

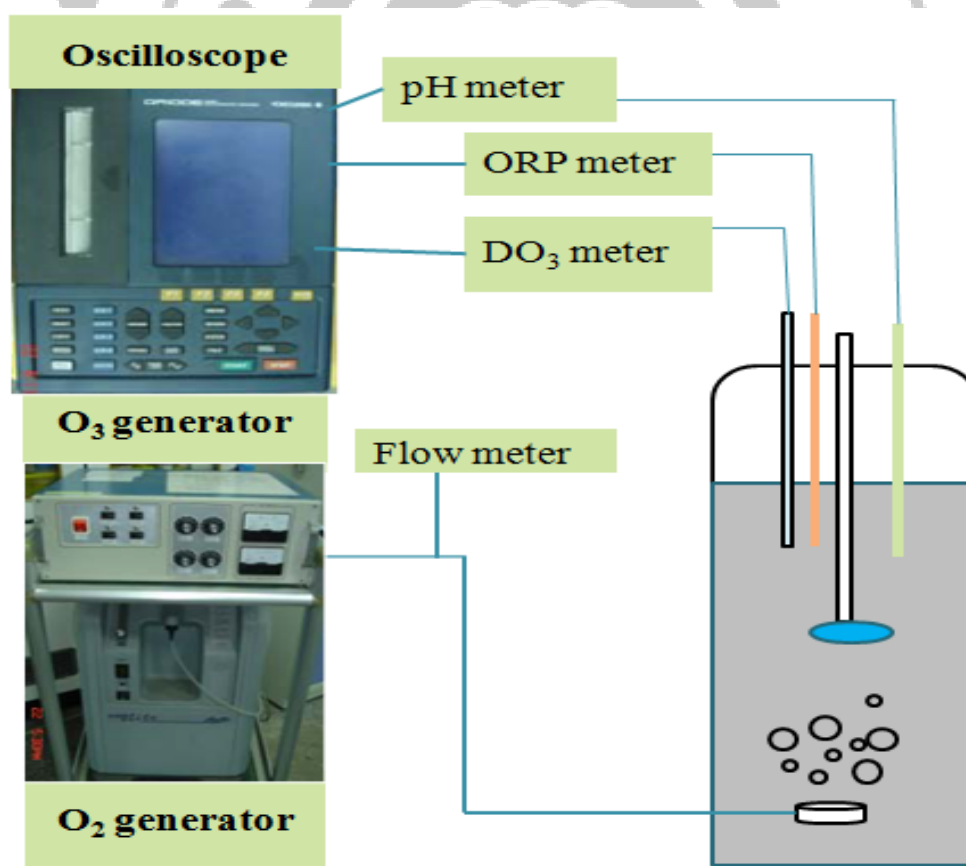


Figure 3.4 Schematic diagrams of ozonation equipment.

Table 3.3 The experimental and online monitor equipment of ozonation system

Equipment	Specification and Operation Conditions
Oscilloscope (Yokogawa, OR100E, Japan)	Channel: Four channel Frequency: 60 MHz Scan rate: 1 Gs/S Data collected: 16,000 data storage per second
Ozone generator (AirSep Corp., KA-1600, USA)	Flow rate: 5000 ± 41 mL/min Ozone production: 0-16 g/hr (Max) Ozone concentration: 10-60 g/m ³ (Max) Oxygen demand: 2~12 L/min Outer diameter: W430×D410×H178 mm Power: 110V, 60Hz, 2.5A
Nitrogen separator (oxygen generator) (AirSep Corp., KA-1600, USA)	Flow rate: 2~5 L/min Outer diameter: W380×D400×H710 mm Power: 110V, 60Hz, 4A
Mixer (Shin kwang, DC-1S, Taiwan)	Rotationl Speed: 80~1,150 rpm Torque: 2.5 kg/cm Motor: 100 W Power: AC 110/220 V, 50/60 Hz

Table 3.4 Experimental instruments

Instruments	Maker, Country
Deionized water machine	MilliQ Academic, USA
Peristaltic Pump (Masterflex)	Cole Palmer Company, USA
Blances Lines (TB-215D)	Denver Instrument, USA
Circulator Oven (DO45)	Deng yng Instrument, Taiwan
Ultrasonic cleaning machine (Power sonic420)	Hwashin technology, South Korea
Hot Plate (UPG-PC-420D)	Corning, USA

3.5 Analytic Methods

3.5.1 Basic water quality analysis

Basic water analysis is referring to NIEA (ROC) and Standard Methods, 21st Ed., (APHA *et al.*, 2005). The items for analysis of this study are pH, temperature, DO, TDS, COD, conductivity, hardness, alkalinity, NH₃-N and ORP were listed in Table 3.5

Table 3.5 Basic water quality analysis items and methods

Items	Methods and Instrument
pH	Electrode method (NIEA W424.50A)*
Temperature	Thermometer method (NIEA W217.51A)*
DO	DO meter
TDS	Conductivity meter
COD	Closed Reflux, Titrimetric methods (Standard Methods 5220C, 21st)**
Conductivity	Conductivity meter method (NIEA W203.51B)*
Hardness	EDTA Titration method (Standard Methods 2340C, 21 st)**
Alkalinity	Titration method (Standard Methods 12320B, 21 st)**
NH ₃ -N	Titrimetric methods (Standard Methods 4500-NH3, 21)**
ORP	ORP meter (Standard Methods 2580B, 21)**

*NIEA method is referred to the Taiwan EPA, R.O.C.

** Standard Methods 21st Ed., by APHA *et al.* (2005)

3.5.2 Disinfection By-Product Formation Potential (DBPFP) Study

The DBPFP used sodium hypochlorite (NaOCl) as culture medium on Te-Chi Reservoir raw water and five species of NOMs extracted from Te-Chi Reservoir raw water which conducted in a 40 mL closed Pyrex glass vials. The initial addition ratio of NaOCl/DOC for each sample was adjusted to 3/1 (Eq. 3.2). The buffer solution in order to maintain the constant pH is mixed 17.025 g KH₂PO₄ and 2.925 g NaOH into 250 mL deionized water before chlorination. Chlorination of the water sample was incubated at 25°C for 7 days.

$$\text{The amount of chlorine added} = \frac{3 \times \text{sample volume (mL)} \times \text{DOC (mg/L)}}{\text{NaOCl concentration (mg/L)}} \quad (\text{Eq. 3.2})$$

3.5.3 Trihalomethanes (THMs)

The THMs analysis was according to the Standard Methods 21th ed., 6232D (APHA *et al.*, 2005) A 5 mL sample was pretreated by using a purge & trap instrument (Eclipse model 4660, O.I. Analytical, USA) and then automatically injected into a gas chromatography equipped with an electron capture detector (GC/ECD) (GC-14B, Shimadzu Co., Kyoto, Japan) connected to a recorder (SIC Chromatocorder 12, Alphatech Corp.,

Tokyo, Japan). Table 3.6 shows that summary of the reagents and equipment's used for THMs analysis.

Table 3.6 Summary of the reagents and equipment used for THMs analysis

Reagent	Cas/Catalog/HS number, Maker, Country
THMs Standards (10^2 mg/L)	Standard # C-188-01, NSI Environmental Solutions, USA.
NaOCl	7681-52-9, J. T. Baker, USA
NaOH	1310-73-2, Merck, Germany
KH ₂ PO ₄	7778-77-0, Merck, Germany
Na ₂ S ₂ O ₃	10102-17-7, Merck, Germany
Equipment	Series Number, Maker, Country
Gas chromatograph	GC-14B, Shimadzu Co., Kyoto, Japan
Electron-Capture Detector	
Recorder	SIC Chromatocorder 12, Alphatech Corp., Tokyo, Japan.
Purge and Trap	Tekmar LSC 2000, Cincinnati, USA

3.5.4 The Characteristics of Fe₃O₄/SiO₂/Pd-Mn

Crystalline phase, surface composition, and elemental analysis were observed by a high resolution scanning electron microscope (HR-SEM and EDS, Hitachi SU8000). The crystalline structure of the catalyst was observed by X-ray diffraction (XRD, Philips). The hysteresis curve of the magnetic catalyst was analyzed by the superconducting quantum interference device vibrating sample magnetometer (SQUID, VSM).

Table 3.7 shows the analytical instruments used in this study.

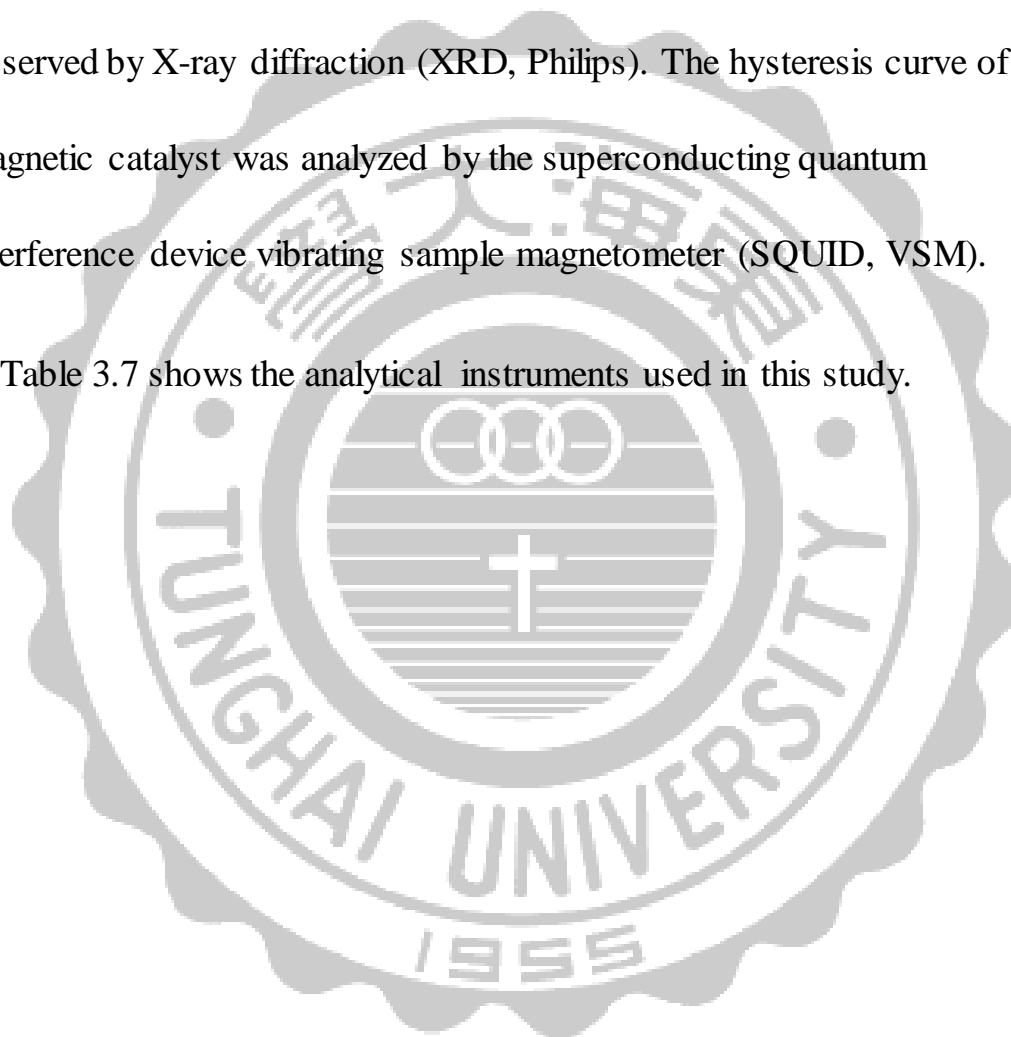


Table 3.7 Analysis instruments of the catalyst (Fe₃O₄/SiO₂/Pd-Mn).

Instrument	Function, Country
Superconducting Quantum Interference Device Vibrating Sample Magnetometer (SQUID VSM)	Hysteresis curve, USA
High Resolution Scanning Electron Microscope and Energy Dispersive Spectrometer (HR-SEM and EDS, HITACHI SU8000)	Crystalline phase, surface composition, and elemental analysis, Japan
Advance X-Ray, PHILIPS X'PERT Pro MPD	Structure identification, Netherlands
Zeta Potential and Submicron Particle Size Analyzers (Beckman Coulter Delsa™ Nano C)	Measure particle size and zeta potential of particles , USA

3.5.5 Absorbance at Wavelength of 254 nm (A_{254}) and Dissolved Organic Carbon (DOC)

NOMs concentration was analyzed using dissolved organic carbon (DOC) and reduction of the UV absorbance at a wavelength of 254 nm (A_{254}). A_{254} was measured with a spectrophotometer (U-2800A, Hitachi, Japan) with a 5 cm quartz cell and DOC was determined by a TOC analyzer (Systematic, 1010, Japan).

Table 3.8 The instrument and reagent for analysis of NOMs.

UV Absorbing (A_{254})	
Instrument	Function, Country
UV/Vis Double Beam spectrophotometer (Hitachi U-2800A)	Quantity of double bond organic matters, Japan

Dissolved organic carbon (DOC)

Instrument	Function, Country
Total organic carbon analyzer (Wet Oxidation-TOC) (1010W, Systematic)	Quantity of dissolved organic carbon, Taiwan

Reagent	Cas/Catalog/HS number, Makers, Country
Na ₂ S ₂ O ₈	7775-27-1, Merck, Germany
H ₃ PO ₄	7664-38-2, Merck, Germany
KHP	877-24-7, Merck, Germany
Na ₂ CO ₃	497-19-8, Merck, Germany

Stock solution: 2.128 g KHP in 1 L reagent water (1,000 mg C/L)

Calibration Equation (2013.04.16):

$$y = 6879.5x + 1340.3 \quad (R^2 = 0.999), \text{ MDL: } 0.05\text{mg/L} \quad (n = 3)$$

3.5.6 Analysis of scavenger

This study applied Coumarin to measure indirectly the hydroxyl radical by High Pressure Liquid Chromatography with UV detection (HPLC-UV) (Jasco Co, UV-975, PU-980, Japan) to analysis Coumarin concentration. The elution solution consisted of methanol, and DI water (V / V =70:30) was used with flow rate of 0.5 mLmin⁻¹. Table 3.9 shows the calibration equation for Coumarin with R² = 0.999 and the M.D.L of 0.03 mg/L after 7 consecutive tests.

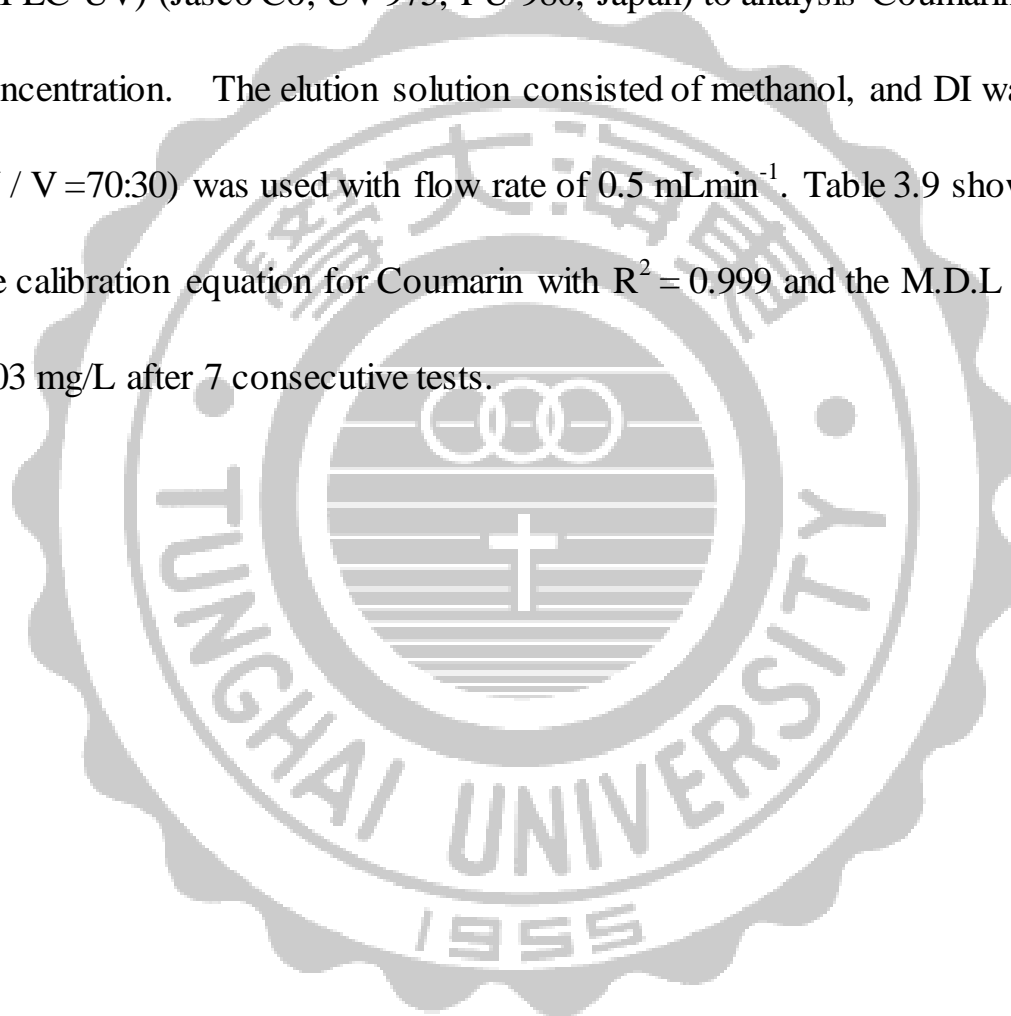


Table 3.9 The instrument and reagent of analysis of hydroxyl radicals scavengers.

Instrument	Specification and Operation Conditions
High performance liquid chromatography (HPLC, Jasco Co., Japan)	Detector: UV-975 Pump: PU-980 Column: Pharmacia C ₂ -C ₁₈ μRPC column ST 4.6/100 Colum volume: 1.66 mL DI water flow rate: 0.5 mL/min Filtration: 0.45 μm membrane Injection loop: 300 μL
Reagent	Cas/Catalog/HS number, Maker, Country
Methanol	67-56-1, Merck, Germany
Coumarin	91-64-5, Merck, Germany

Calibration equation of coumarin (2013.09.27):

$$y = 94634x - 2424.1, R^2 = 0.999, MDL = 0.03 \text{ mg/L (n= 7)}$$

Chapter 4 Results and Discussions

4.1 The characteristic of Te-Chi Reservoir

4.1.1 Water quality of Te-Chi Reservoir

The Te-Chi Reservoir provides the main water source to the greater metropolitan Taichung region of 3 million populations. Furthermore, the mountain near Te-Chi Reservoir, there are planted fruit and used a lot of organic fertilizer would be flowed into reservoirs. The excess fertilizer around the reservoir is flowing into it with top soil and caused the degradation of reservoir water quality. Table 4.1 showed the analytic at data of Te-Chi Reservoir during 2007 and 2013. The pH value is between 7.3 and 8.5, which is slightly higher than the average pH (6.0-8.5) from the reservoirs in Taiwan. The alkalinity is 162 mg CaCO₃/L higher than last year. During the past few years, the higher alkalinity is caused by carbon dioxide (CO₂) of atmosphere and decomposed of organic matter in waters. The DO value is 7.54 mg/L, which it's higher than the previous level of 7.19-7.28 mg/L and caused by the algae blooming. While TDS value is 154 mg/L, which is far below the standard TDS value of 500 mg/L. The value of COD, DOC and hardness are 5 mg/L, 3.41 mg/L and 122 mg CaCO₃/L, respectively. While, the state standard on average

values for hardness values is 300 g CaCO₃/L for Taiwan drinking water standard (EPA , 2014). The TDS, COD, DOC and hardness values are higher than last year. The range of temperature is from 22.9 to 23.8 °C and the variation of temperature was influence for pH, DO and alkalinity.



Table 4.1 The water quality parameters of Te-Chi Reservoir raw water in recent years.

Item	pH	Temp °C	DO mg/L	TDS mg/L	COD mg/L	DOC mg/L	Hardness mg CaCO ₃ /L	Alkalinity mg CaCO ₃ /L	NH ₃ -N mg/L
Taiwan EPA std.	6.5-8.5	-	-	-	-	-	≤ 300	≤ 50	≤ 0.1
2007.08	8.18	22.9	5.93	47	13	1.06	121	130	0.1
2008.08	7.38	18.9	10.0	258	12	1.03	130	180	0.12
2009.07	8.51	23.7	7.19	219	4	3.39	125	177	0.3
2010.08	8.14	23.0	7.27	211	4	3.10	127	152	0.4
2011.08	7.44	23.8	7.65	149	6	3.51	134	179	0.4
2012.08	7.36	22.5	7.28	144	4	3.24	128	142	0.3
2013.08	8.44	23.5	7.54	154	5	3.41	125	162	0.3

* The drinking water resources quality standard of Taiwan EPA (2014)

4.1.2 The organic fractions ratio in NOMs of Te-Chi Reservoir

This study adapts the method of DAX-8 to extract the NOMs into five organic species from Te-Chi raw water for investigating the distribution characteristics of it (Crou'e *et al.*, 1993).

The five fractions include: humic acids (HAs), fulvic acids (FAs), hydrophobic base (HPO-B), hydrophobic neutral (HPO-N) and hydrophilic fraction (HPI-F). The percentage of five organic species has been shown in Figure 4.1 from Te-Chi Reservoir in 2013. The HPO-B which is caused by drift wood, blade and mud was brought into reservoir by rain erosion, therefore HPO-B was higher than HPI-F. In this study, the percentage of HAs, FAs, hydrophobic neutrals (HPO-N), hydrophobic bases (HPO-B) and hydrophilic fractions (HPI-F) are 11.7%, 26.8%, 21.2%, 3.4% and 29.8%, respectively. This study used the Te-Chi raw water to conduct the decomposing study.

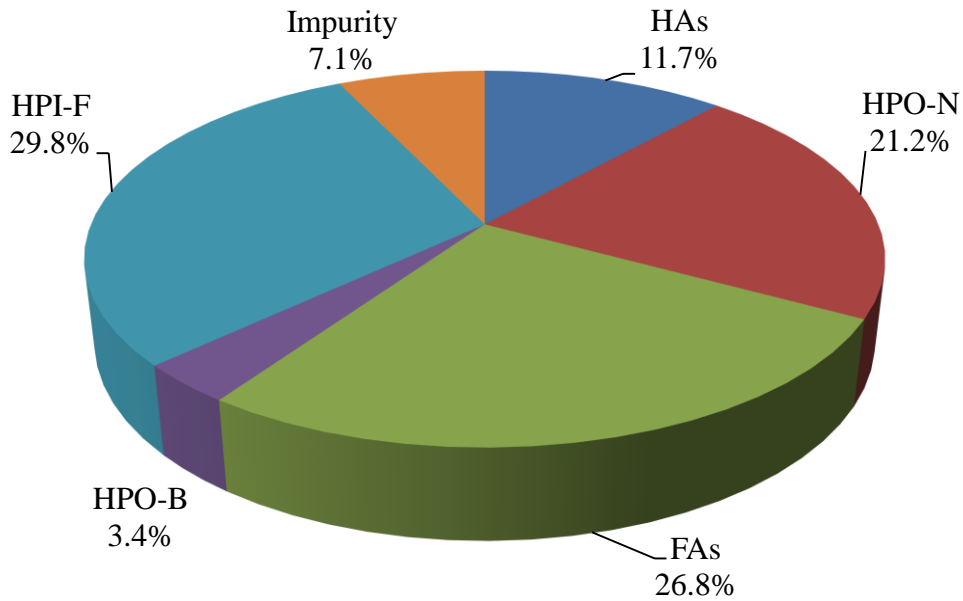


Figure 4.1 The percentage of five (HAs, FAs, HPO-N, HPO-B and HPI-F) of organic fractions extracted from Te-Chi reservoir raw water in 2013 (Separated the organic compounds by DAX-8 Resin, Crou'e *et al.*, 1993).

The distributions of NOMs from Te-Chi Reservoir in recent years are shown in Table 4.2. HPOA (humic acids and fulvic acids) would generate high DBPFP easily. Recent years, the typhoon brought heavy mud slide and tree into Te-Chi Reservoir, the water body contained a lot of hydrophobic matters degraded by tree. During the sampling time in 2013, few floating materials presented on the water surface, therefore, the HAs may be lower than the previous findings. Comparing with the recent years, the percentage of HAs and FAs increased from 10.7% to 11.7%;

and 22.1% to 26.8 %.The more hydrophobic fractions in water, the more DBPFP may be generated during the disinfection process.



Table 4.2 The percentage distribution of Te-Chi Reservoir NOMs (% of DOC) in recent years (2006-2010).

Reference, Fraction (%)	HAs	FAs	Hydrophobic neutrals	Hydrophobic bases	Hydrophilic fractions
2006.08	29.5	19.5	37.9	2.9	10.2
2008.08	47.4	4.7	42.2	0.7	5
2009.07	10.7	22.1	20.8	3.8	42.6
2010.08	10.8	25.4	23.2	4.0	34.9
2011.08	12.4	21.6	22.3	4.1	38.3
2012.08	10.3	24.8	24.1	4.6	35.7
This study 2013.08	11.7	26.8	21.2	3.4	29.8

4.2 Characterization of the assembled catalysts

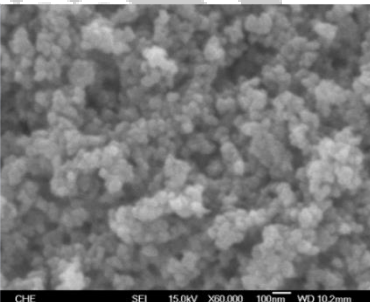
The $\text{Fe}_3\text{O}_4/\text{SiO}_2/\text{Pd-Mn}$ preparation had been attempted under many conditions in order to obtain high content of Pd-Mn. An SEM image (Figure 4.2 (b)) confirmed that both Pd-Mn had been coated on silica successfully in a condition of ethanol as solvent and calcined in 350°C SEM. Oppositely, the image in Figure 4.2 (a) shows the Mn had not been coated on the catalyst prepared by water as solvent. Therefore, this study adapts ethanol as solvent to conduct the catalyst preparation.

Figure 4.3 shows the X-ray diffraction patterns of $\text{Fe}_3\text{O}_4/\text{SiO}_2/\text{Pd-Mn}$, which reflection peaks of Palladium/manganese dioxide appeared at $2\theta \doteq 37.2, 40.06, 58$ and 68.10 degree. Ha *et al.*, (2013) and Liang *et al.*, (2008) noted that Palladium peak was appeared at 2θ of 40.03 and 68.10 rdegree; manganese dioxide peak was appeared at 2θ of 37.2 and 58 degree, which are very closed to the Palladium/manganese dioxide peaks obtained in this study. From the XRD analysis (Figure 4.3), it was shown a stable output of catalyst assembled in this study.

Figure 4.4 showed the zeta potential of Palladium/manganese catalyst low from 21.56 to -1.03 mV. The catalyst the pH point of zero charge (pHpzc) is found to be 10.9 .

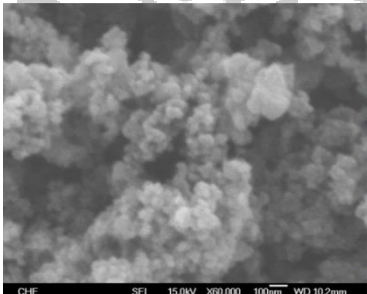
Figure 4.5 shows that catalyst presented the super paramagnetic phenomenon at room temperature (25°C) and the magnetization was about 42.7, 23.6 and 22.5 emu/g. Comparison of previous studies (Feng *et al.*, (2010), Li *et al.*, (2010), Wang *et al.*, (2011) and Lin, (2012)), the particles synthesized ($\text{Fe}_3\text{O}_4/\text{SiO}_2/\text{Pd-Mn}$) in this study are with higher magnetization and smaller particle size (40-50nm) than previous works (Table 4.3). Figure 4.5 shows the catalyst can be easily recovered by magnets.

Element	Weight%	Atomic%
O K	47.32	69.23
Si K	21.97	18.31
Fe K	28.61	11.99
Pd L	2.10	0.46
Totals	100.00	



CHE SEI 15.0kV X60,000 100nm WD 10.2mm

(a) in water



Element	Weight%	Atomic%
O K	43.28	66.09
Si K	22.16	19.28
Mn K	1.66	0.74
Fe K	30.50	13.34
Pd L	2.40	0.55
Totals	100.00	

CHE SEI 15.0kV X60,000 100nm WD 10.2mm

(b) in ethanol

Figure 4.2 SEM image of synthesis of particle calcined in 350°C (a) Pd-activated MnCO_3 in water (b) Pd-activated MnCO_3 in ethanol.

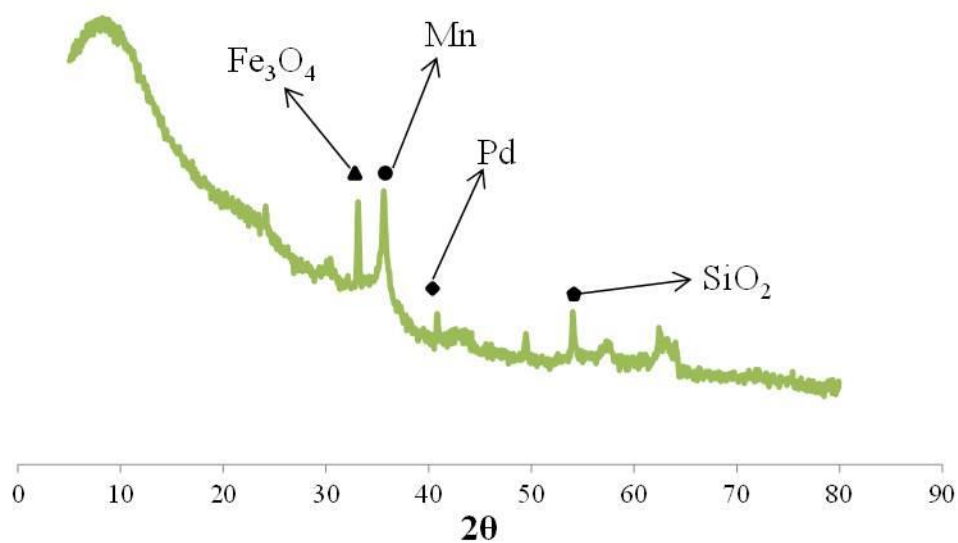


Figure 4.3 XRD spectra of $\text{Fe}_3\text{O}_4/\text{SiO}_2/\text{Pd-Mn}$

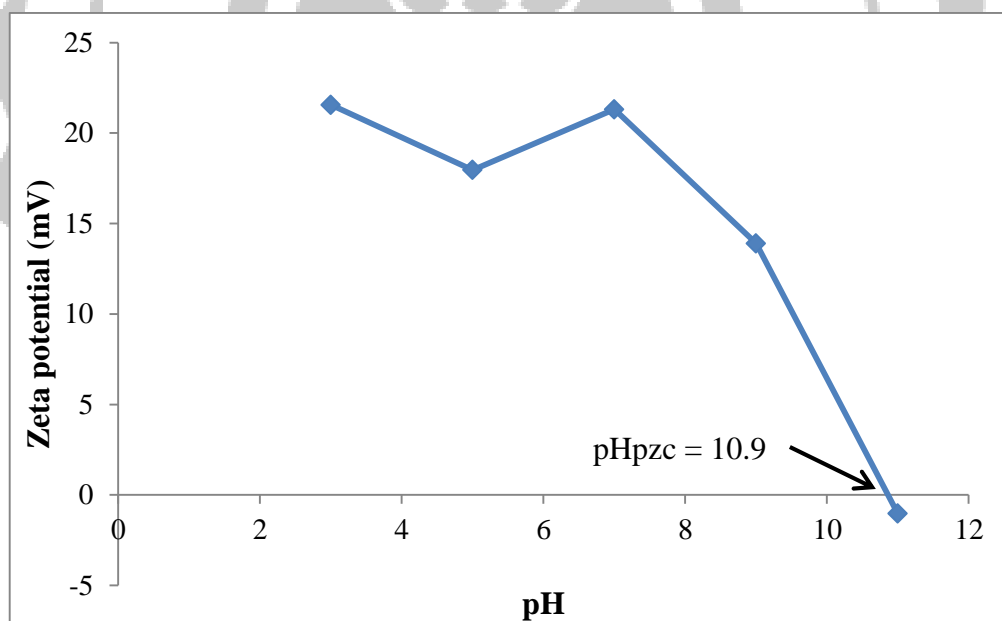


Figure 4.4 The zeta potential values of $\text{Fe}_3\text{O}_4/\text{SiO}_2/\text{Pd-Mn}$ (pH 3, 5, 7, 9 and 11) and with pH_{PZC} of 10.9.

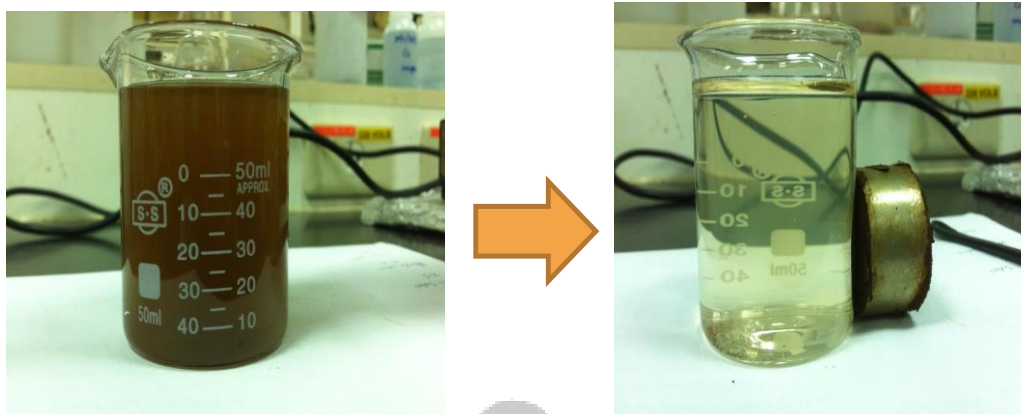


Figure 4.5 The magnet attracts the catalysts in solution.

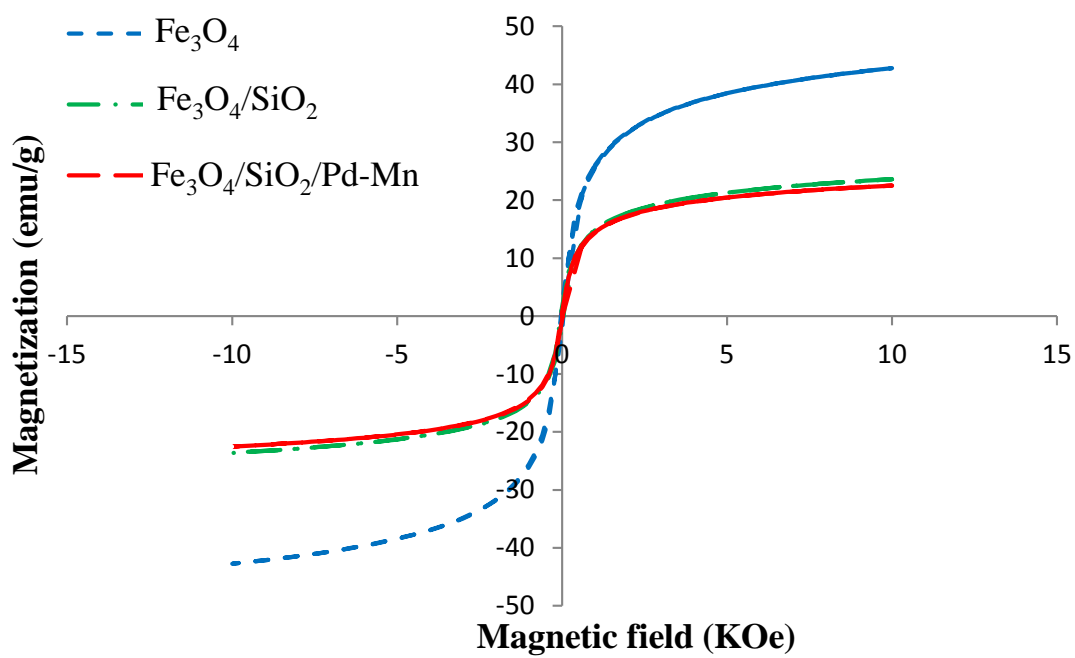


Figure 4.6 Field-dependent magnetization hysteresis of $\text{Fe}_3\text{O}_4/\text{SiO}_2/\text{Pd-Mn}$ at 25°C

Table 4.3 The comparison of magnetic particles in different references.

Reference	Particle structure	Particle size (nm)	Magnetization (emu/g)
Feng <i>et al.</i> (2010)	Fe ₃ O ₄ /SiO ₂ -GPTMS-Asp -Co	215	15.0
Li <i>et al.</i> (2010)	Fe ₃ O ₄ /SiO ₂ /Au	130	17.1
	Fe ₃ O ₄ /SiO ₂ /Au-Ag	470	15.0
Wang <i>et al.</i> (2011)	Fe ₃ O ₄ /SiO ₂ /PbS	545	26.0
Yuan <i>et al.</i> (2012)	Fe ₃ O ₄ /SiO ₂ /meso-TiO ₂	325	38.7
Lai and Chen (2013)	Fe ₃ O ₄ /SiO ₂ /Van-LaB ₆	245	17.68
This study (2015)	Fe₃O₄/SiO₂/Pd-Mn	50-100	22.5

4.3 Catalytic ozonation of raw water

4.3.1 Effect of dosage

Figures 4.7 and 4.8 provide A_{254} and DOC decomposition profiles under catalytic ozonation of organic compounds in different dosages. NOMs are compounds that compose the benzene groups which are produced by refractory decomposition in an ozone system. A_{254} decomposition had only slight efficiency (23%) reached at 30 min in sole ozonation case. Catalytic ozonation of raw water was done with 0.25, 0.5, 1 and 1.5 g/L of $\text{Fe}_3\text{O}_4/\text{SiO}_2/\text{Pd-Mn}$ were investigated. The highest decomposition of A_{254} (70%) and DOC removal (52%) were both observed at the dosage of 1 g/L catalyst case. Additional dosage of catalyst (1.5 g/L) was disadvantageous in enhancing the degradation and mineralization of raw water because it was overloaded with steric hindrance proposed by Liu *et al.*, (2012) and may decrease the surface area of catalyst.

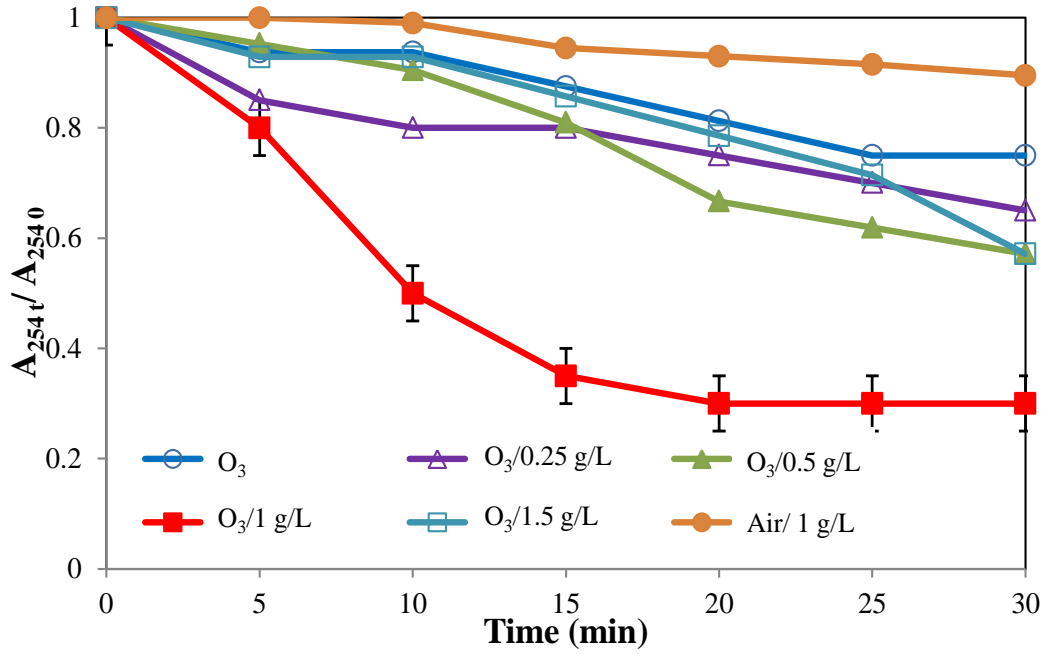


Figure 4.7 The decomposition of A_{254t}/A_{2540} in different catalyst dosage (0, 0.25, 0.5, 1.0 and 1.5 g/L) (O_3 concentration of 0.6 mg/L and pH 7.5).

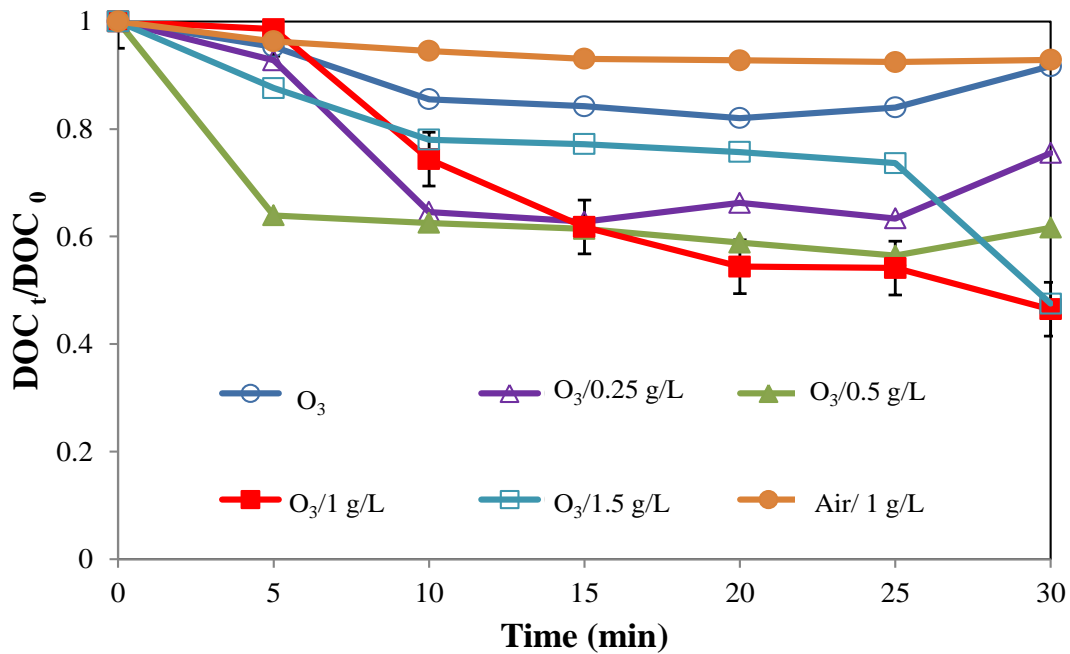


Figure 4.8 The mineralization of DOC_t/DOC_0 in different catalyst dosage (0, 0.25, 0.5, 1.0 and 1.5 g/L) (O_3 concentration of 0.6 mg/L and pH 7.5).

4.3.2 Effect of pH

Figures 4.9 and 4.10 provide the decomposition with A_{254} and DOC for catalytic ozonation of NOMs compounds in different pHs. The former is a reliable indicator of the aromatic content of the potential for DBP formation (Patsios *et al.*, 2013) while water pH is one of the most important factors in catalytic ozonation. Catalytic ozonation of raw water pHs were conducted with pHs of 3, 5, 7, 9 and 11. In 5 minutes, the removal reached 50% in pH 9, while in pH 11 the removal reached 60% - 80% in 30 minutes. The decomposition has higher efficiency in high pH than low pH. Figure 4.9 shows the catalytic ozonation in pH 11 is efficient and reached 90% while the mineralization in other pHs still maintained only 50%.

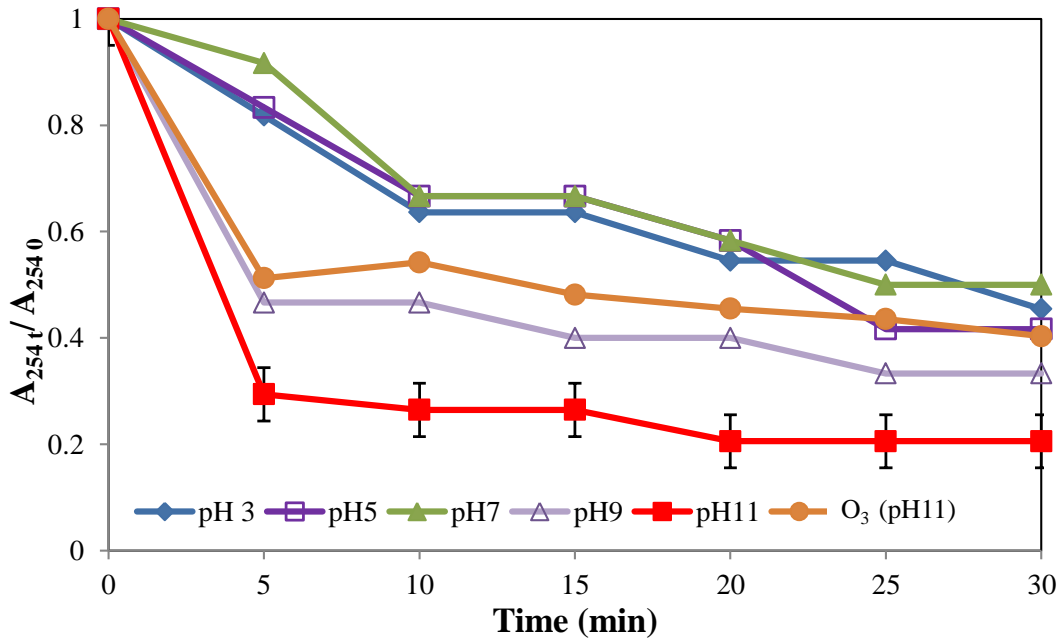


Figure 4.9 The decomposition of rate A_{254t}/A_{2540} in different pHs (3, 5, 7, 9 and 11) (O_3 concentration of 0.6 mg/L and catalyst dosage of 1 g/L).

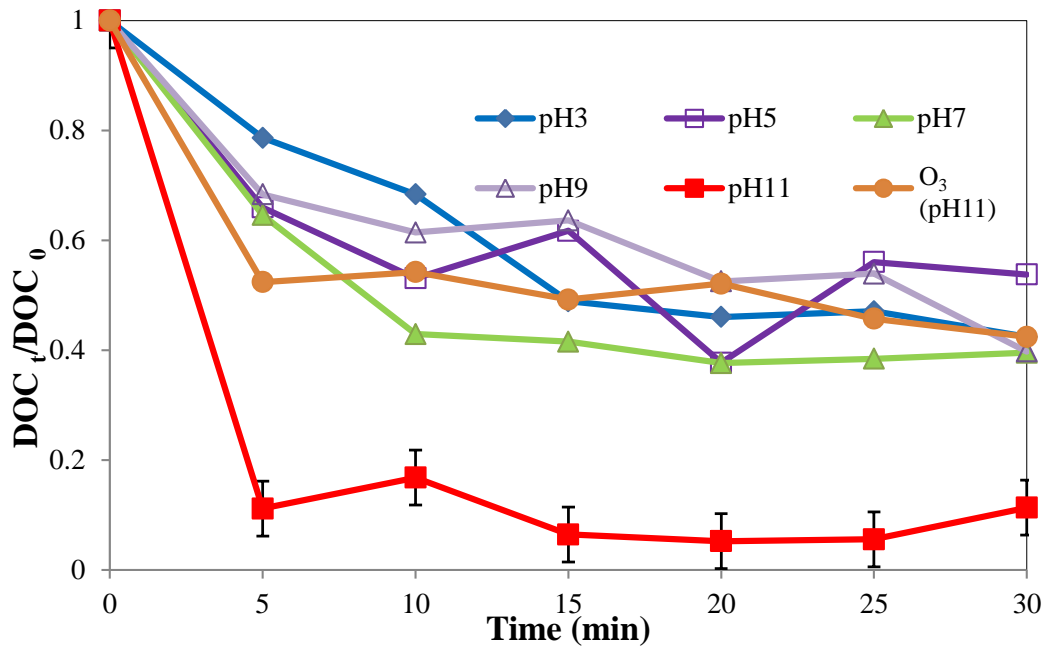


Figure 4.10 The mineralization of rate DOC_t/DOC_0 in different pHs (3, 5, 7, 9 and 11) (O_3 concentration of 0.6 mg/L and catalyst dosage of 1 g/L).

4.3.3 The k_d value of catalytic ozonation under first-order reaction

Figures 4.11 and 4.12 show the first-order reaction kinetic rate (k_d) value of different dosages and pHs. The k_d value was $2.7 \times 10^{-2} \text{ min}^{-1}$ with a dosage of 1 g/L and was the highest k_d values compared with other groups. However, under various pH cases (3, 5, 7, 9, 11) k_d values were 2.91, 1.8, 2.8, 2.4 and $6.5 \times 10^{-2} \text{ min}^{-1}$, respectively. The k_d value of pH 11 which is greater than that other reports. It also indicates that the k_d value of $\text{Fe}_3\text{O}_4/\text{SiO}_2/\text{Pd-Mn}$ is 1.5 times than that of $\text{Fe}_3\text{O}_4/\text{SiO}_2/\text{Ag}$. The results showed that $\text{Fe}_3\text{O}_4/\text{SiO}_2/\text{Pd-Mn}$ are efficient catalyst to decompose retardant NOMs raw water.

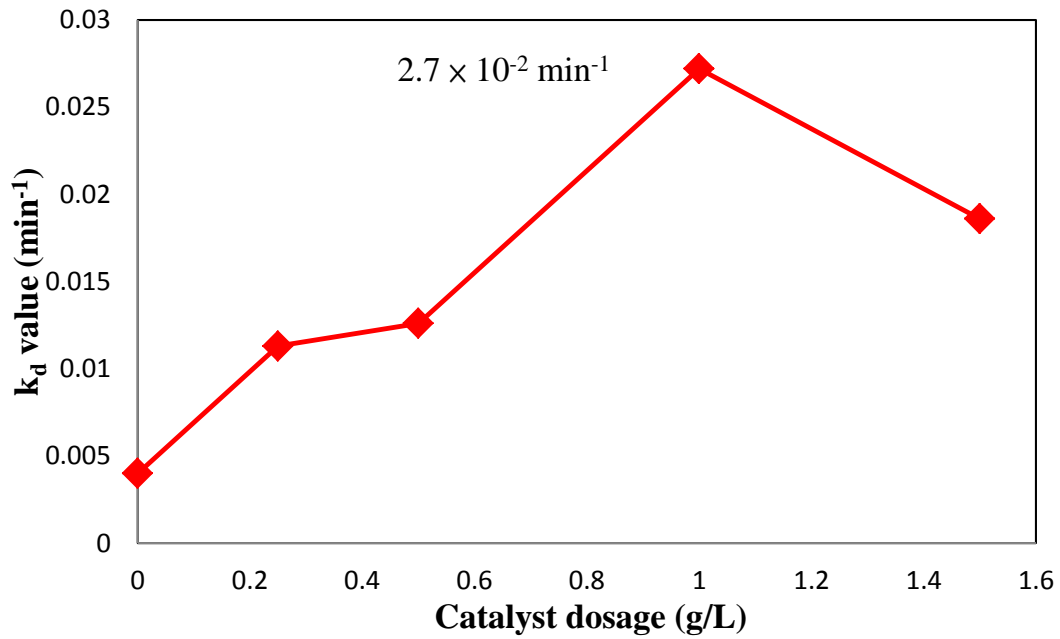


Figure 4.11 The k_d value of catalytic ozonation in different dosage (0, 0.25, 0.5, 1.0 and 1.5 g/L) under first-order reaction (based upon DOC).

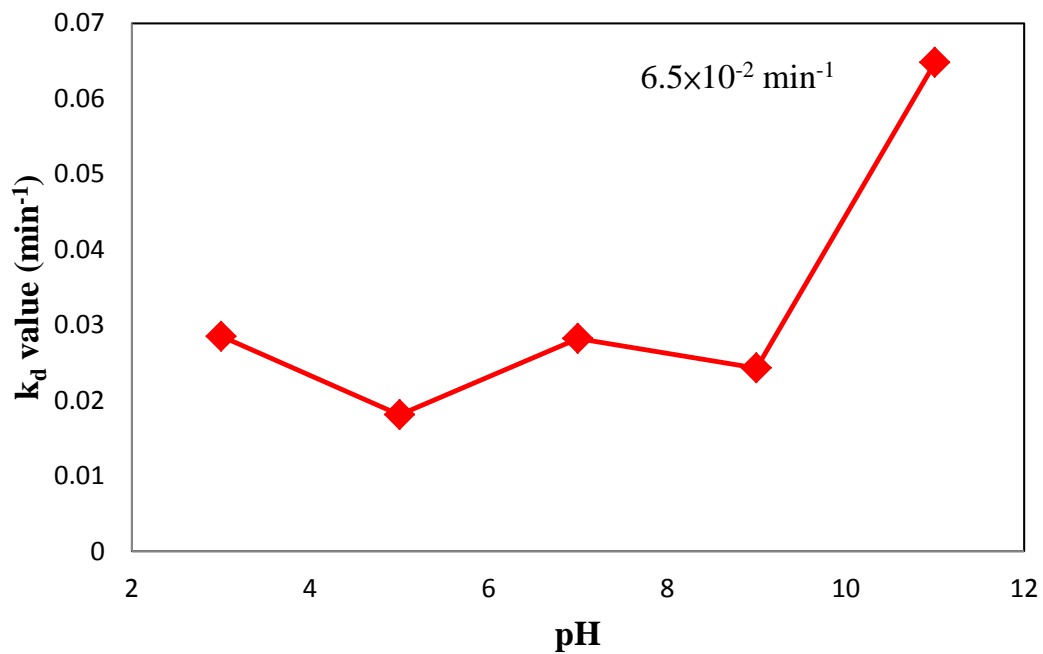
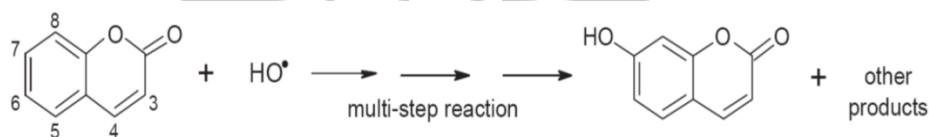


Figure 4.12 The k_d value of catalytic ozonation in different pHs under first-order reaction (based upon DOC).

4.3.4 Catalytic ozonation of coumarin in different pH conditions

pH is an important factor to understand the mechanisms of catalytic ozonation. Coumarin is used as a scavenger to capture free radical in solution. Figures 4.13 and 4.14 shows that pH 11 has the highest more efficient to decompose coumarin in this study with pH: 3, 5, 7, 9 and 11 and k values were 1.4, 1.3, 2.1, 4.6 and $6.0 \times 10^{-2} \text{ min}^{-1}$, respectively. Even though coumarin had been depletion almost 90%, the remained amount was still enough to keep probing in 30 minutes. The results were similar to former group which was catalytic ozonation of raw water. Pd-Mn as catalyst of ozonation in condition of pH 11 is more powerful oxidant contributed to hydroxyl radical, stronger oxidant. Coumarin was a molecule that had been known to form the fluorescent 7-hydroxycoumarin by reaction with hydroxyl radicals in aqueous solutions showed in Eq.1 (Lout *et al.*, 2005).



Eq. 4.1

Figure 4.15 shows the formation of 7-hydroxycoumarin, was monitored during catalytic ozonation of coumarin. At pH 11, reaction

resulted in significant the by-product: 7-hydroxycoumarin at 20 minute during reaction time. Then, 7-hydroxycoumarin would decrease due to subsequent reaction of with ozone or perhaps catalytic action (Patsios *et al.*, 2013).

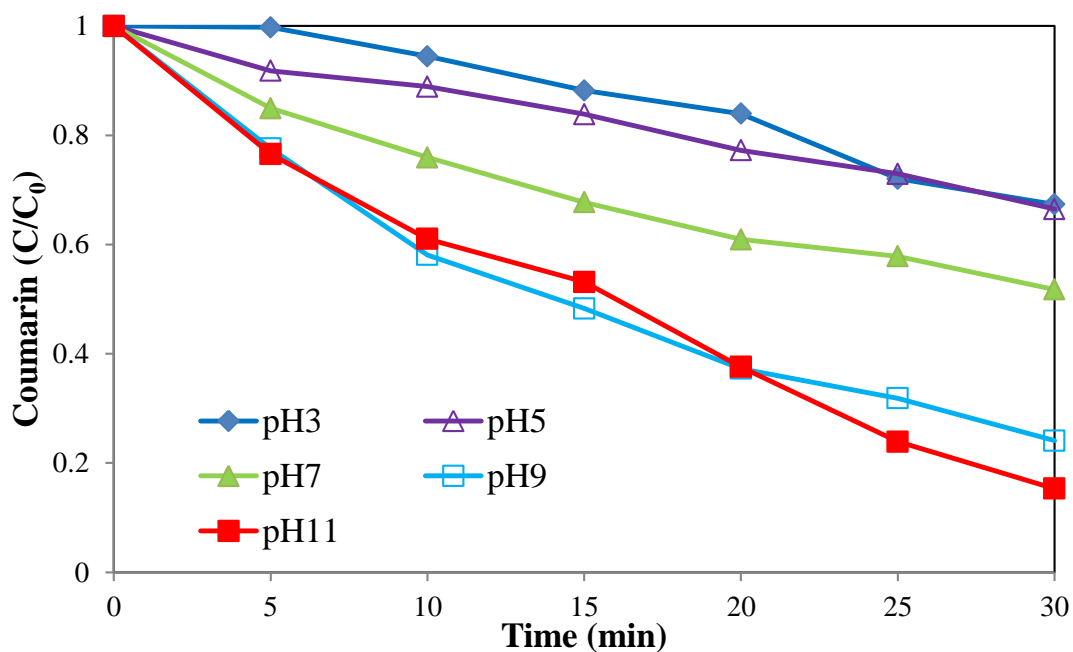


Figure 4.13 The coumarin removal in the catalytic ozonation under various pHs (O_3 concentration of 0.6 mg/L and catalyst dosage of 1 g/L).

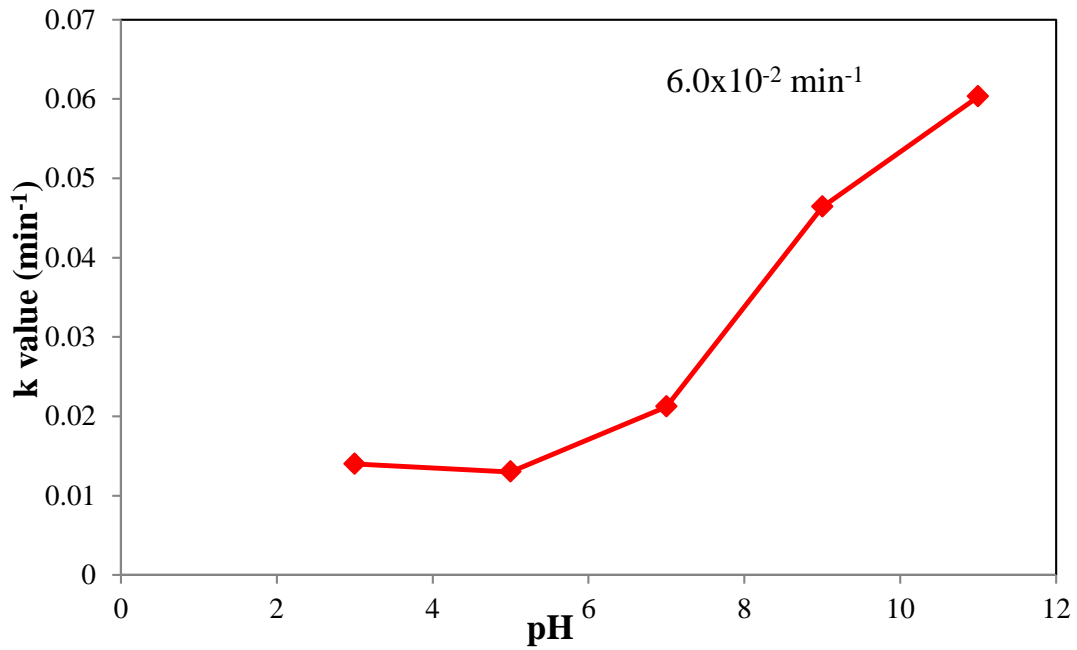


Figure 4.14 The k value of coumarin decomposition in different pH (3, 5, 7, 9 and 11) under first-order reaction.

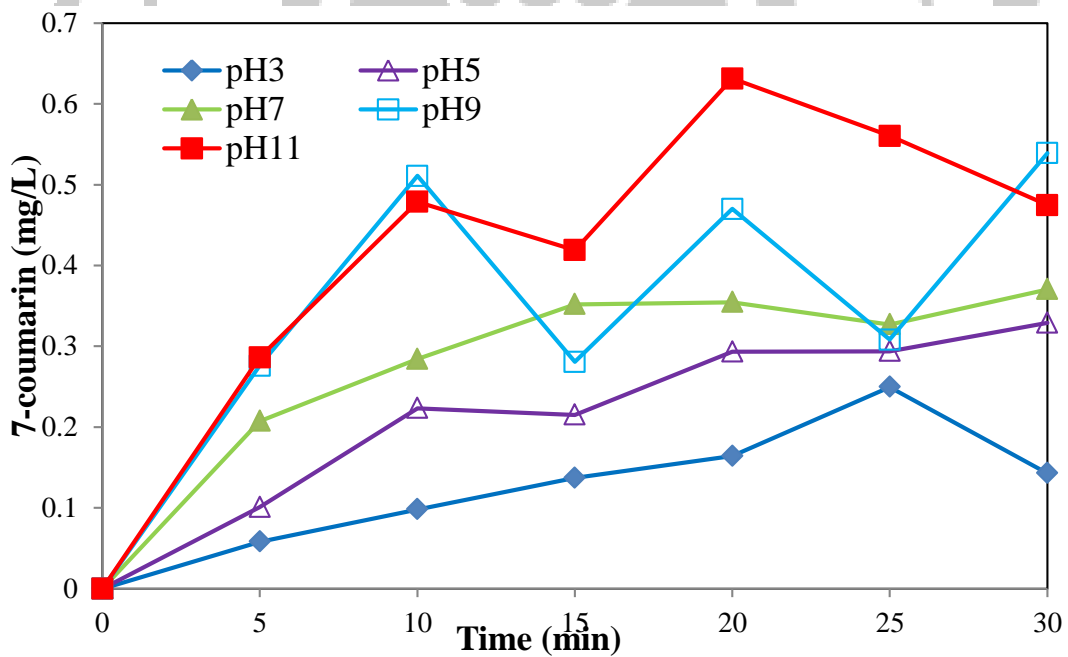


Figure 4.15 The byproduct 7-coumarin in the catalytic ozonation under various pHs (O_3 concentration of 0.6 mg/L and catalyst dosage of 1 g/L).

Table 4.4. The comparison of coumarin removal rates (k) for different catalyst under ozonation (O₃:1.6 mg/L).

Reference	pH	Ozonation system	Catalyst dose (gL ⁻¹)	k (min ⁻¹)
Lu (2011)	3	O ₃ /(Fe ₃ O ₄ /SiO ₂ /Co)	1.0	4.6x10 ⁻²
Chen (2012)	3	O ₃ /(Ag/AC)	0.5	5.8x10 ⁻²
	6.2	O ₃ /Al ₂ O ₃	6	6.1x10 ⁻²
	6.2	O ₃ /Z1000H	2	6.0x10 ⁻²
Ikhlaiq(2012)	6.2	O ₃ /Z25H	4	4.6x10 ⁻²
	6.2	O ₃ /Z1000H	2	6.0x10 ⁻²
This study (2015)	11	O ₃ /(Fe ₃ O ₄ /SiO ₂ /Pd-Mn)	1.0	6.0x10 ⁻²

4.4 The reduction of THMFPs

Chlorination is a main disinfection process in drinking water for most countries, while the NOMs in reservoirs could be formed THMs.

The decomposition of NOMs was in sole ozonation and catalytic ozonation and then would be chlorination after treatment for investigating the formation of THMFPs shown in figure 4.16. Decreases in THMFPs were around 38% by sole ozonation and 74% by catalytic ozonation.

Hydroxyl radicals are more powerful oxidant for refractory compounds than ozone alone. Catalytic ozonation was almost twice times efficiency

of decomposition to sole ozonation contributed to more generation of hydroxyl radicals.

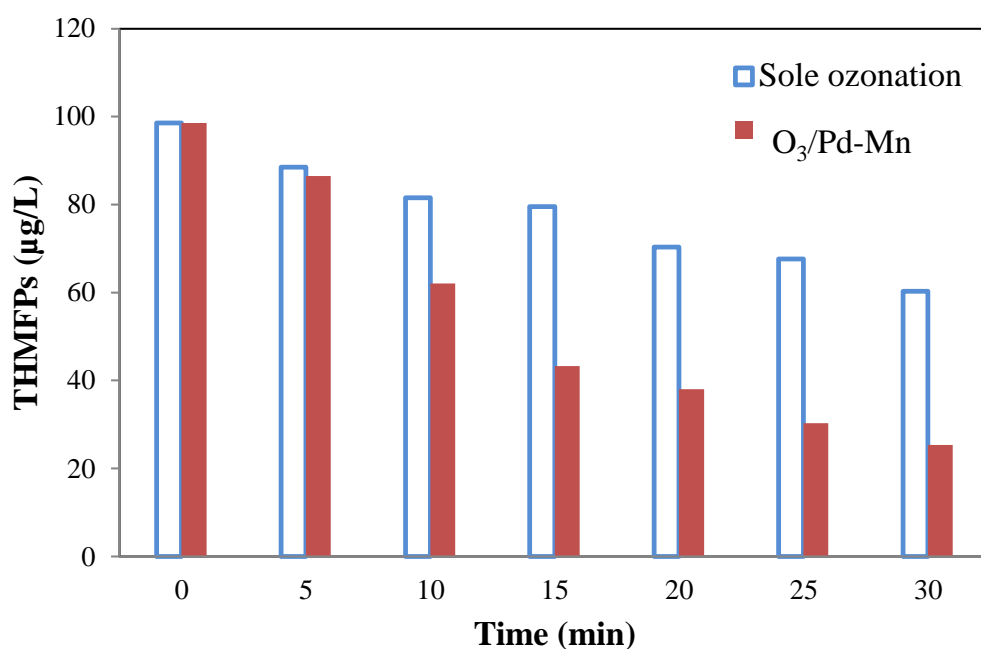


Figure 4.16 The reduction of THMFPS by sole ozonation and catalytic ozonation (Fe₃O₄/SiO₂/Pd-Mn).

4.5 Modeling catalyst reaction

The Nernst equation has been used to simulate the redox reaction (Chang *et al.*, 2004; Hancock *et al.*, 2004). Nicoli *et al.*, (2004) suggested that the ORP value represents the information about the real oxidation/reduction ability of a molecule and its prevalent form (oxidized

or reduced) in the system.

Theoretically, the concentration of both the reactants and products can be represented by the measurement of A_{254} . The decrease A_{254} means the mineralization of organic matter content in the water.

Therefore, organic compounds ($C_xH_yO_z$) can be replaced by A_{254} for detecting decomposed organic compounds. The pH can be measured in the redox reaction equation. The typical Nernst equation can be expressed as Eq. 4.2

$$E = E^0 + (RT/nF) \ln ([\text{Oxi}]/[\text{Red}]) \dots \dots \dots \text{Eq. 4.2}$$

Therefore Nernst equation is obtained as follow:

$$\text{ORP}_{A_{254}} = 27,240 - 14755.3 \ln [A_{254}] - 2486.91 \text{ pH} + 2.64 \ln [\text{THMFPS}] \dots \dots \dots \text{Eq. 4.3}$$

The model regression shows a satisfactory R–square value of 0.996 for THMFPS (Figure 4.18). In this study, the Nernst model can be used to simulate and control the THMFPS removal in the future.

Figure 4.18 showed that the relationship between THMFPS and ORP was obviously positive correlation. THMFPS were decreased to 20 ppb that ORP in system was necessary to be increased up to 700mV. The R–

square value of 0.996 indicates the measured ORP curve can properly by the form of modified Nernst Equation.

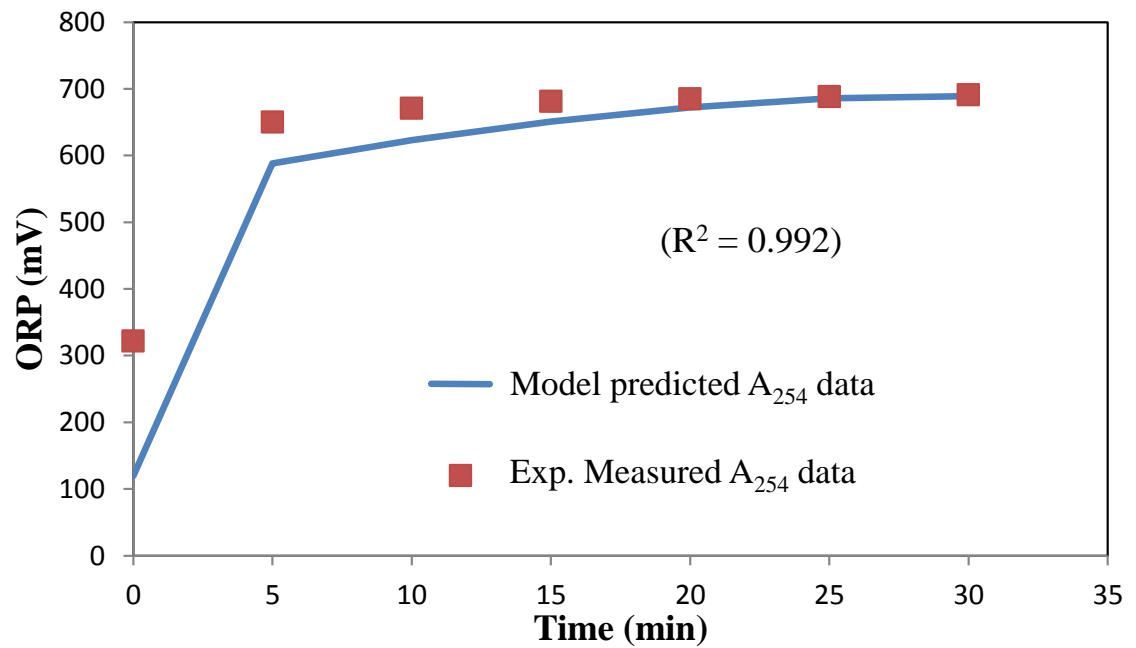


Figure 4.17 The Nernst model simulations of A₂₅₄ profiles of catalytic ozonation of Te-Chi Reservoir raw water.

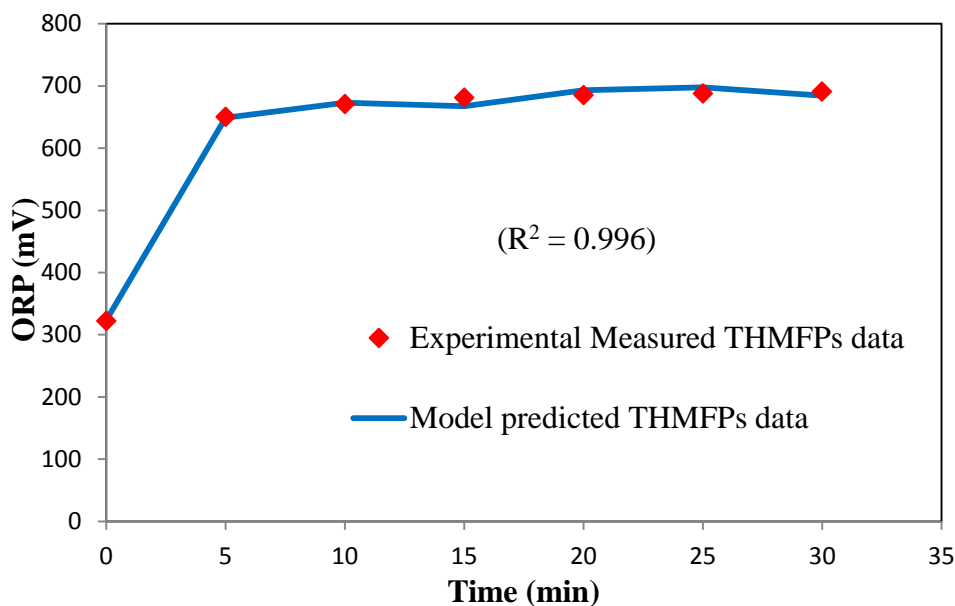


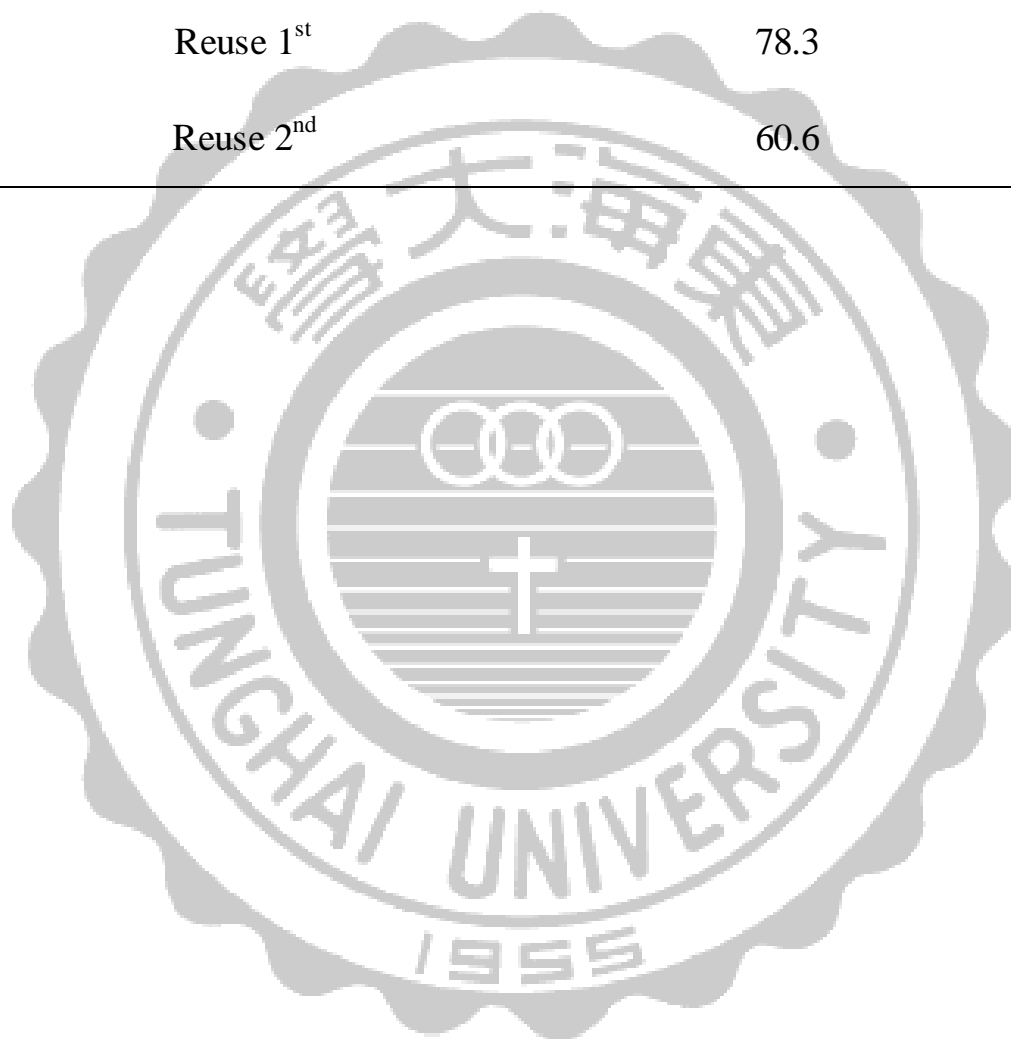
Figure 4.18 The Nernst model simulation of THMFPs profiles of catalyst ozonation of Te-Chi Reservoir raw water.

4.6 Reuse of the catalyst

The stability and reusability of the catalyst are one of the economic factors in catalyzed reactions. The reusability of the $\text{Fe}_3\text{O}_4/\text{SiO}_2/\text{Pd-Mn}$ catalyst was investigated by reuse of the catalyst in ozonation experiments. All of the catalyst reuse experiments were carried out under identical reaction conditions. The results (Table 4.5) showed that $\text{Fe}_3\text{O}_4/\text{SiO}_2/\text{Pd-Mn}$ recovery after two times still retains efficiency of 60-80% when decomposing humic acid.

Table 4.5 Reusability of $\text{Fe}_3\text{O}_4/\text{SiO}_2/\text{Pd-Mn}$ to decompose NOMs under ozonation.

Reuse times	Efficiency removal (%)
Raw	89
Reuse 1 st	78.3
Reuse 2 nd	60.6

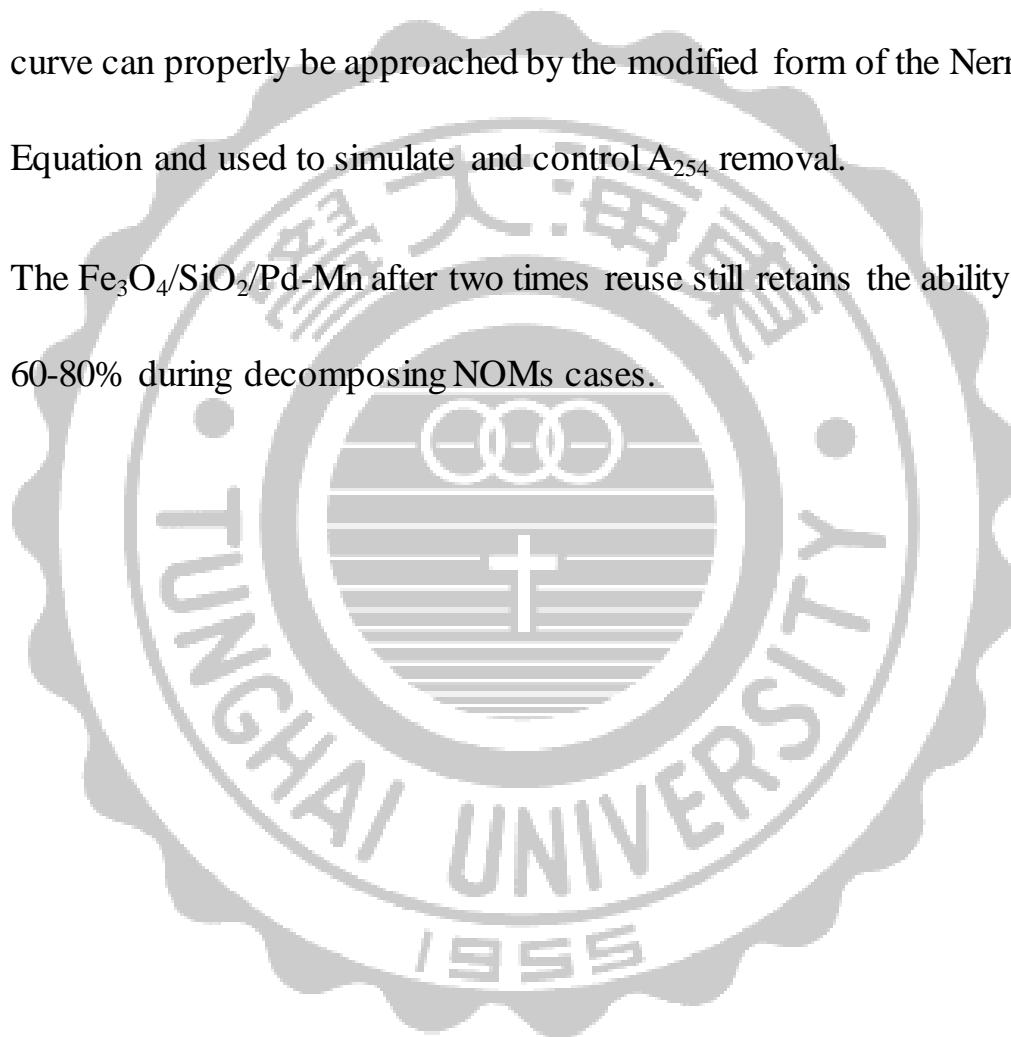


Chapter 5 Conclusions and Suggestions

5.1 Conclusions

1. The catalyst ($\text{Fe}_3\text{O}_4/\text{SiO}_2/\text{Pd-Mn}$) was synthesized and observed by SEM, EDS and XRD analysis in this study. The Pd-Mn had been coated on silica satisfactorily in condition of ethanol as solvent and calcined at 350°C .
2. Under the chosen conditions (1 g/L catalyst dosage, pH 11), $\text{Fe}_3\text{O}_4/\text{SiO}_2/\text{Pd-Mn}$ displays high catalytic activity on ozonation of raw water.
3. The first-order reaction kinetic rate constant (k) implies that the highest coumarin removal rate ($6.0 \times 10^{-2} \text{ min}^{-1}$) is under the dosage of 1 g/L and pH 11 than that in other studies and the amount still remained to keep probing hydroxyl radicals in 30 minutes.
4. The intermediate by-product: 7-hydroxycoumarin were indicated the effects of hydroxyl radical on catalytic. 7-hydroxycoumarin was generated mostly in catalytic ozonation under pH 11.

5. The decomposition of THMFPs had an efficiency of 75 % in Pd-Mn catalytic ozonation under the condition of pH 11 and dosage of 1 g/L.
6. The comparison of the predicted model and the on-line monitored Nernst equation under the redox system show that the measured ORP curve can properly be approached by the modified form of the Nernst Equation and used to simulate and control A_{254} removal.
7. The $Fe_3O_4/SiO_2/Pd-Mn$ after two times reuse still retains the ability of 60-80% during decomposing NOMs cases.



5.2 Suggestions

1. In order to reused catalysts maintain the effective catalysis, it can attempt to different conditions of synthesized preparation.



References

- Acero J.L and von Gunten., (2001), “Characterization of oxidation processes: ozonation and the AOP O_3/H_2O_2 ”, Am Water Works Ass, Vol. 93, pp. 90-100.
- Adams, F.V., Nxumalo, E.N., Krause, R.W.M., Hoek, E.M.V., Mambaa, B.B., (2014), “Application of polysulfone/cyclodextrin mixed-matrix membranes in the removal of natural organic matter from water”, Physics and Chemistry of the Earth, Vol.67–69, p.71–78
- APHA, AWWA and WEF, (2005), “Standard methods for examination of water and wastewater, 21st Edition”, American Public Health Association, Washington D.C., USA
- Badis, A., Ferradji, F.Z., Boucherit, A., Fodil, D., Boutoumi, H., (2010), “Removal of natural humic acids by decolorizing actinomycetes isolated from different soils (Algeria) for application in water purification”, Desalination, Vol. 259, pp. 216-222.
- Baghoth, S.A, Sharma, S.K, Amy, G.L., (2011) “Tracking natural organic matter (NOM) in a drinking water treatment plant using fluorescence excitation-emission matrices and PARAFAC”, Water Research, Vol.45, pp.797-809.
- Beltrán, F.J., Rivas, F.J., Montero-De-Espinosa, R., (2005), “Iron type catalysts for the ozonation of oxalic acid in water”, Water Research, Vol. 39, p. 3553-3564.
- Bougeard, C.M.M., Goslan, E.H., Jefferson, B., Parsons, S.A., (2010), “Comparison of the disinfection by-product formation potential of treated waters exposed to chlorine and monochloramine”, Water Research Vol. 44, p. 729-740.
- Buffle J.A.E., (1997) “Les substances humiques et leurs interactions avec les ions minéraux”, Proc. Commission d’hydrologie appliquée de AGHTM l’Université d’Orsay, pp. 3-10.

Carbajo, M., Rivas, F.J., Beltrán, F.J., Alvarez, P., Medina, F., (2006), “Effects of different catalysts on the ozonation of pyruvic acid in water”, *Ozone: Science and Engineering*, Vol. 28, p. 229-235.

Chang, Cheng-Nan, Hong-Bang Cheng and Allen C. Chao., (2004), “Applying the Nernst Equation To Simulate Redox Potential Variations for Biological Nitrification and Denitrification Processes”, *Environ. Sci. Technol.*, Vol. 38, pp.1807-1812

Chowdhury, Shakhawat, Rodriguez, Manuel J., Sadiq, Rehan, Serodes, Jean., (2011) “Modeling DBPs formation in drinking water in residential plumbing pipes and hot water tanks”, *Water Research*, Vol.45, pp.377-347.

Cortes, S., Sarasa, J., Ormad, P., Gracia, R., Ovelleiro, J.L., (2000), “Comparative efficiency of the systems O_3 /high pH and O_3 /catalyst for the oxidation of chlorobenzenes in water”, *Ozone: Science and Engineering*, Vol. 22, p. 415-426.

Croué, J.P, Lefebvre E, Martin B, Legube B., (1993), “Removal of dissolved hydrophobic and hydrophilic organic substances during coagulation/flocculation of surface waters”, *Water Science and Technology*, Vol. 27, pp. 143-152.

Feng, Guodong, Hu, Daodao, Yang, Lei, Cui, Yali, Cui, Xin-ai, Li, Hong, (2010), “Immobilized-metal affinity chromatography adsorbent with paramagnetism and its application in purification of histidine-tagged proteins”, *Separation and Purification Technology*, Vol.27, pp.253-260

Gracia, R., Aragües, J.L., Ovelleiro, J.L., (2000), “Study of the catalytic ozonation of humic substances in water and their ozonation byproducts”, *Ozone: Science and Engineering*, Vol. 18, p. 195-208.

Gunten U.V., (2003), “Ozonation of drinking water: part I. Oxidation kinetics and product formation”, *Water Research*, Vol. 37, pp. 1443-1467.

Gunten U.V., (2003), “Ozonation of drinking water: part II. Oxidation kinetics and product formation”, *Water Research*, Vol. 37, pp. 1443-1467.

Ha, The An, Van Man Tran and My Loan Phung Le, (2013), “Nanostructured composite electrode based on manganese dioxide and carbon Vulcan-carbon nanotubes for an electrochemical supercapacitor”, *Advances in Natural Sciences: Nanoscience and Nanotechnology*, Vol.4, pp.03504 (5pp)

Hancock, J.T., Desikan R., Neill S.J., Cross A.R., (2004), “New equations for redox and nano-signal transduction”, *Journal of Theoretical Bio.*, Vol.226, pp.65-68.

Heisig, Christopher, Zhang, Weimin, Oyama, S. Ted., (1997), “Decomposition of ozone using carbon-supported metal oxide catalysts”, *Applied Catalysis B: Environmental*, Vol. 14, pp. 117-129.

Hewes, C. G, Davinson R.R, (1972), “Renovation of waste water by ozonation”, *Water AIChE Symposium Series*, Vol. 69, p. 71.

Hoigne, J. and Staehelin, J., (1982), “Decomposition of Ozone in Water: Rate of Initiation by Hydroxide Ions and Hydrogen Peroxide”, *Environmental Science and Technology*, Vol.16, p. 676.

Ikhlaq, Amir, (2012), “Catalytic ozonation for the removal of anthropogenic organic contaminants in water”, *University of Huddersfield Repository*, Doctoral dissertation.

Ikhlaq, Amir, Brown, David R., Kasprzyk-Hordern, Barbara, (2012), “Mechanisms of catalytic ozonation on alumina and zeolites in water: Formation of hydroxyl radicals”, *Applied Catalysis B: Environmental*, Vol. 123–124, pp. 94-106.

Jones, D.B., Saglam A., Song H., Karanfil T., (2012), “The impact of bromide/iodide concentration and ratio on iodinated trihalomethane formation and speciation”, *Water Research*, Vol. 46, p. 11-20.

Karnik, B.S., Davies, S.H., Baumann, M.J., Masten, S.J., (2005), “The effects of combined ozonation and filtration on disinfection by-product formation”, *Water Research*, Vol. 39, p. 2839-2850

Kasprzyk-Hordern, Barbara, Ziólek, Maria, Nawrocki, Jacek, (2003), “Catalytic ozonation and methods of enhancing molecular ozone reactions in water treatment”, *Applied Catalysis B: Environmental*, Vol. 46, pp. 639-669.

Ksenofontova, M.M. , Mitrofanova, A.N., Mamleeva, N.A., Pryakhin, A.N., Lunin, V.V., (2003), “Ligninsulfonate Ozonation in the Presence of Transition Metal Ions”, *Ozone: Science and Engineering*, Vol. 25, p. 505-512.

Lai, Bo Hung and Chen, Dong Hwang, (2013), “ancomycin-modified $\text{LaB}_6@ \text{SiO}_2/\text{Fe}_3\text{O}_4$ composite nanoparticles for near-infrared photothermal ablation of bacteria”, *Acta Biomaterialia*, Vol.9, pp.7573-7579

Langlais, B., Reckhow D.A., Brink D.R., (1991), “Ozone in Water Treatment: Application and Engineering”, Lewis Publishers, Chelsea, MI.

Lau, T.K., Chu W., Graham N., (2007), “Reaction pathways and kinetics of butylated hydroxyanisole with UV, ozonation, and UV/ O_3 processes”, *Water Research*, Vol. 41, p. 765-774.

Legube, B. and Leitner, N.K.V., (1999), “Catalytic ozonation: a promising advanced oxidation technology for water treatment”, *Catalysis Today*, Vol. 53, p. 61-72.

Li, Huanan, Xu , Bingbing, Qi, Fei, Sun, Dezhi, Chen, Zhonglin., (2014), “Degradation of bezafibrate in wastewater by catalytic ozonation with cobalt doped red mud: Efficiency, intermediates and toxicity”, *Applied Catalysis B: Environmental* , Vol. 152-153, p. 342-351.

Li, L., Ye W., Zhang Q., Sun F., Lu P., Li X., (2009), “Catalytic ozonation of dimethyl phthalate over cerium supported on activated carbon”, *Journal of Hazardous Materials*, Vol. 170, p. 411-416.

- Li, Ling, Eugene S.G. Choo, Xiaosheng Tang, Jun Ding, Junmin Xue, (2010), “Ag/Au-decorated Fe₃O₄/SiO₂ composite nanospheres for catalytic applications”, *Acta Materialia*, Vol.58, pp.3825-3831
- Liang, Xi, Chang-Jun Liu and Penghu Kauai, (2008), “Selective oxidation of glucose to gluconic acid over argon plasma reduced Pd/Al₂O₃”, *Green Chem*, Vol.10, pp.1318-1322
- Liu, Hao, Deng, Huiping, Shi, Jun., (2012) “Activated carbon and cerium supported on activated carbon applied to the catalytic ozonation of polycyclic aromatic hydrocarbons”, *Journal of Molecular Catalysis A: Chemical*, Vol.363, pp.101-107.
- Liu, Wenbo, Zhao, Yanmei, Chow, WK, Christopher, Wang, Dongsheng, (2011), “Formation of disinfection byproducts in typical Chinese drinking water”, *Journal of Environmental Sciences*, Vol. 23, pp. 897-903.
- Liotta, L.F., Gruttadauria M., Carlo G. Di, Perrini G., Librando V., (2009), “Review-Heterogeneous catalytic degradation of phenolic substrates: Catalysts activity”, *Journal of Hazardous Materials*, Vol. 162, p. 588 - 606.
- Louit, Guillaume, Foley, Sarah, Cabillic, Julie, Coffigny, Herve, Taran, Frederic, Valleix, Alain, Renault, Jean Philippe, Pin, Serge., (2005) “The reaction of coumarin with the OH radical revisited: hydroxylation product analysis determined by fluorescence and chromatography”, *Radiation Physics and Chemistry*, Vol.72, pp.119-124.
- Matheswaran, M., Balaji, S., Chung, S.J., Moon, I.S., (2007), “Studies on cerium oxidation in catalytic ozonation process: A novel approach for organic mineralization”, *Catalysis Communications*, Vol. 8, p. 1497-1501.
- Matilainen, Anu, Gjessing E.T., Lahtinen T., Hede L., Bhatnagar A., Sillanpää M., (2011), “Review - An overview of the methods used in the characterization of natural organic matter (NOM) in relation to drinking water treatment”, *Chemosphere*, Vol. 83, p. 1431-1442.

Marhaba, T.F., Kanokkantapong V., Panyapinyophol B., Wattanachira S. and Pavasant P., (2006), "Characterization of Natural Organic Matter Fractionation for Bangkok Water Source", Thai Env. Eng., Journal Vol. 19, p. 17-27.

Nawrocki, J., Kasprzyk-Hordern B., (2010), "Review-The efficiency and mechanisms of catalytic ozonation", Applied Catalysis B: Environmental, Vol. 99, p. 27 -42.

Nicoli, M.C., Toniolo R., Anese M., (2004), "Relationship between redox potential and chain-breaking activity of model systems and foods", Food Chemistry, Vol.88, pp.79.83.

Orge, C.A., Órfão, J.J.M., Pereira, M.F.R., (2012), "Composites of manganese oxide with carbon materials as catalysts for the ozonation of oxalic acid", Journal of Hazardous Materials, Vol. 213-214, pp. 133-139.

Patsios, S. I., Sarasidis, V.C., Karabelas, A.J., (2013), "A hybrid photocatalysis-ultrafiltration continuous process for humic acids degradation", Separation and Purification Technology, Vol. 104, pp. 333-341

Polshettiwar, V., Luque, R., Fihri, A., Zhu, H.B., Bouhrara, M., Basset, J.M., (2011), "Magnetically recoverable nanocatalysts", Chemical Reviews, Vol. 111, pp. 3036-3075.

Rosal, R., Rodriguez A., Gonzalo M. S. and Garca-Calvo E., (2008), "Catalytic ozonation of naproxen and carbamazepine on titanium dioxide", Applied Catalysis B: Environmental, Vol. 84, p. 48-57.

Rosal, Roberto, Gonzalo, Maria S., Rodriguez, Antonio, Garcia-Calvo, Eloy, (2010), "Catalytic ozonation of fenofibric acid over alumina-supported manganese oxide", Journal of Hazardous Materials, Vol. 183, pp. 271-278.

Rosenfeldt, E.J., Linden K.G., Canonica S., von Gunten U., (2006), “Comparison of the efficiency of •OH radical formation during ozonation and the advanced oxidation processes O₃/H₂O₂ and UV/H₂O₂”, *Water Research.* , Vol. 42, p. 3695 - 3704.

Rupa A.V., Vaithyanathan R. and Sivakumar T., (2011), “Noble metal modified titania catalysts in the degradation of Reactive Black 5: a kinetic approach”, *Water Science & Technology*, Vol.64, p.1040–1045.

Sánchez-Polo, M., Rivera-Utrilla, J., (2004), “Ozonation of 1,3,6-naphthalenetrisulfonic acid in presence of heavy metals”, *Journal of Chemical Technology and Biotechnology*, Vol. 79, p. 902-909.

Skoumal, M., Cabot P.-L., Centellas F., Arias C., R.M. Rodríguez, Sauleda R., Brillas E., (2001), “Mineralization of aniline and 4-chlorophenol in acidic solution by ozonation catalyzed with Fe²⁺ and UVA light”, *Applied Catalysis B: Environmental*, Vol. 29, p. 135–145.

Stevenson F.J., (1982) “Humus Chemistry”, *Water Research*, John Wiley & Sons, New York.

Trapido, M., Veressinina, Y., Munter, R., Kallas, J., (2005), “Catalytic ozonation of m-dinitrobenzene”, *Ozone: Science and Engineering*, Vol. 27, p. 359-363.

Valencia, Sergio, Juan M. Mari ´n , Gloria Restrepo , Fritz H. Frimmel., (2014) “Evaluation of natural organic matter changes from Lake Hohloh by three-dimensional excitation emission matrix fluorescence spectroscopy during TiO₂/UV process”, *Water Research*, Vol.51, pp.124-133.

Valdesa, Hector, Farfan, Victor J., Manoli, Jorge A., Zaror, Claudio A., (2009) “Catalytic ozone aqueous decomposition promoted by natural zeolite and volcanic sand”, *Journal of Hazardous Materials*, Vol.165, pp.915-922.

Wang, Yan, Zhang, Hui, Chen, Lu, (2011), “Ultrasound enhanced catalytic ozonation of tetracycline in a rectangular air-lift reactor”, *Catalysis Today*, Vol.175, pp.283-292

Wu, C.-H., Kuo, C.-Y., Chang, C.-L., (2008) “Decolorization of C.I. Reactive Red 2 by catalytic ozonation processes”, *Journal of Hazardous Materials*, Vol. 153, p. 1052-1058.

Yuan, Qing, Li, Nan, Geng, Wangchang, Chi, Yue, Li, Xiaotian, (2012), “Preparation of magnetically recoverable $\text{Fe}_3\text{O}_4@\text{SiO}_2@\text{meso-TiO}_2$ nanocomposites with enhanced photocatalytic ability”, *Materials Research Bulletin*, Vol.47, pp.2396-2402

Yu, Quan Wei, Hao Pan, Ming Zhao, Zhimin Liu, Jianli Wang, Yaoqiang Chen, Maochu Gong., (2009), “Influence of calcination temperature on the performance of Pd-Mn/ $\text{SiO}_2\text{-Al}_2\text{O}_3$ catalysts for ozone decomposition”, *Journal of Hazardous Materials*, Vol. 172, pp.631-634.

Zhao, Hui, Dong, Yuming, Wang, Guangli, Jiang, Pingping, Zhang, Jingjing, Wu, Lina, Li, Kun, (2013), “Novel magnetically separable nanomaterials for heterogeneous catalytic ozonation of phenol pollutant: NiFe_2O_4 and their performances”, *Chemical Engineering Journal*, Vol. 219, pp. 295-302.

Zazouli, M.A., Nasser S., Mahvi A.H., Gholami M., Mesdaghinia A.R. and Younecian M., (2008), “Studies on Rejection and Fouling of Polyamide Reverse Osmosis Membrane in the Treatment of Water Solutions Containing Humic Acids”, *World Applied Sciences Journal*, Vol. 3 (3), p. 434-440.

Zularisam, A.W., Ismail A.F., Salim R., (2006), “Behaviours of natural organic matter in membrane filtration for surface water treatment-a review”, *Desal*, Vol. 194, p. 211-231.

Zularisama, A.W., Ahmada, Anwar, Sakinah, Mimi, Ismail, A.F., Matsuura, T., (2011), “Role of natural organic matter (NOM), colloidal particles, and solution chemistry on ultrafiltration performance”, *Separation and Purification Technology*, Vol. 78, pp. 189-200.

江佳玲，(2006)，“製備磁性催化劑與應用於臭氧反應之探討”，東海大學環境科學與工程學系碩士論文。

洪詩涵，(2007)，“氫氧自由基對臭氧反應影響之探討”，東海大學環境科學與工程學系碩士論文。

蔡宜穎，(2009)，“應用 ORP 與氫氧自由基探討臭氧和臭氧超音波反應機制”，東海大學環境科學與工程學系碩士論文。

張勳鍊，(2010)，“以實驗設計和氫氧自由基探討臭氧反應對於天然有機物降解和消毒副產物減量”，東海大學環境科學與工程學系碩士論文。

呂理維，(2011)，“利用磁性金屬臭氧催化劑降解水中消毒副產物”，東海大學環境科學與工程系碩士論文。

林世軒，(2012)，“改良磁性奈米銀觸媒進行異相催化臭氧去除水中腐植酸之研究”，東海大學環境科學與工程系碩士論文。

陳貴樺，(2012)，“應用活性炭/銀催化劑去除水中有機物質”，東海大學環境科學與工程系碩士論文。